

This discussion paper is/has been under review for the journal *Atmospheric Chemistry and Physics (ACP)*. Please refer to the corresponding final paper in *ACP* if available.

**Aerosol  
characterization in  
N-Africa, NE-Atlantic,  
M. Basin and M. East**

S. Basart et al.

# **Aerosol characterization in Northern Africa, Northeastern Atlantic, Mediterranean Basin and Middle East from direct-sun AERONET observations**

**S. Basart<sup>1</sup>, C. Pérez<sup>1</sup>, E. Cuevas<sup>2</sup>, J. M. Baldasano<sup>1,3</sup>, and G. P. Gobbi<sup>4</sup>**

<sup>1</sup>Earth Sciences Department, Barcelona Supercomputing Center-Centro Nacional de Supercomputación, BSC-CNS, Barcelona, Spain

<sup>2</sup>Izaña Atmospheric Research Center, Meteorological State Agency of Spain (AEMET), Santa Cruz de Tenerife, Spain

<sup>3</sup>Environmental Modelling Laboratory, Technical University of Catalonia, Barcelona, Spain

<sup>4</sup>Institute of Atmospheric Sciences and Climate, ISAC-CNR, Rome, Italy

Received: 23 January 2009 – Accepted: 6 March 2009 – Published: 24 March 2009

Correspondence to: S. Basart (sara.basart@bsc.es)

Published by Copernicus Publications on behalf of the European Geosciences Union.

Title Page

Abstract

Introduction

Conclusions

References

Tables

Figures

⏪

⏩

◀

▶

Back

Close

Full Screen / Esc

Printer-friendly Version

Interactive Discussion

## Abstract

We provide an atmospheric aerosol characterization for North Africa, Northeastern Atlantic, Mediterranean and Middle East based on the analysis of quality-assured direct-sun observations of 39 stations of the AEROSOL ROBOTIC NETWORK (AERONET) which include at least an annual cycle within the 1994–2007 period. We extensively test and apply the recently introduced graphical method of Gobbi and co-authors in order to track and discriminate different aerosol types and quantify the contribution of mineral dust. The method relies on the combined analysis of the Ångström exponent ( $\alpha$ ) and its spectral curvature. Plotting data in these coordinates allows to infer aerosol fine mode size ( $R_f$ ) and fractional contribution ( $\eta$ ) to total Aerosol Optical Depth (AOD) and separate AOD growth due to fine-mode aerosol humidification and/or coagulation from AOD growth due to the increase in coarse particles or cloud contamination. Our results confirm the robustness of this graphical method. Large mineral dust is the most important constituent in Northern Africa and Middle East; and under specific meteorological conditions, its transport to Europe is observed from spring to autumn. Small pollution particles are abundant in sites close to urban and industrial areas of Continental and Eastern Europe and Middle East; as well as, important contributions of biomass burning are observed in the sub-Saharan region in winter. Dust is usually found to mix with these fine, pollution aerosols.

## 1 Introduction

Aerosols frequently exhibit widely varying optical properties over time due to diffusion and aging processes such as coagulation, humidification, scavenging by precipitation and gas to particle phase conversion (Schuster et al., 2006). These processes combined with varying source strengths and advections by local to synoptic meteorological processes create a dynamic atmospheric constituent affecting climate, environment and public health (IPCC, 2007).

ACPD

9, 7707–7745, 2009

## Aerosol characterization in N-Africa, NE-Atlantic, M. Basin and M. East

S. Basart et al.

Title Page

Abstract

Introduction

Conclusions

References

Tables

Figures

◀

▶

◀

▶

Back

Close

Full Screen / Esc

Printer-friendly Version

Interactive Discussion

---

**Aerosol  
characterization in  
N-Africa, NE-Atlantic,  
M. Basin and M. East**S. Basart et al.

---

[Title Page](#)[Abstract](#)[Introduction](#)[Conclusions](#)[References](#)[Tables](#)[Figures](#)[⏪](#)[⏩](#)[◀](#)[▶](#)[Back](#)[Close](#)[Full Screen / Esc](#)[Printer-friendly Version](#)[Interactive Discussion](#)

Ground-based aerosol remote sensing does not provide global coverage; however, its numerous spectral measurements of solar radiation are well suited to reliably and continuously derive aerosol optical properties. In spite of high temporal and spatial aerosol variability, there are a rather limited number of general categories of aerosol types with distinctly different optical properties which are associated with different sources and emission mechanisms.

Aerosol optical depth (AOD) at wavelength  $\lambda$  is the standard parameter measured by sunphotometers as those operating in AERONET (Holben et al., 1998). The AOD spectral dependence is mainly driven by the scattering efficiency and can be expressed by means of the classical Ångström's equation ( $\text{AOD}(\lambda) \sim \lambda^{-\alpha}$ ) (Ångström, 1929). In the solar spectrum, the Ångström exponent ( $\alpha$ ) is a good indicator of the dominant size of the atmospheric particles. AOD generated mainly by submicron particles are characterized by  $\alpha > 1$  whereas supermicron aerosols would lead to  $\alpha < 1$ . As shown in numerous studies (e.g. Eck et al., 1999; Reid et al., 1999; Holben et al., 2001; Dubovik et al., 2002; Smirnov et al., 2002a; Pace et al., 2006; Kaskaoutis et al., 2007), the combined use of the AOD and  $\alpha$  allows to distinguish between different aerosol types. As opposite to clean atmospheres ( $\text{AOD} < 0.15$ ) dominated by oceanic aerosols, high values of AOD are characteristic of turbid atmospheres affected by biomass burning, dust plumes or urban pollution (Dubovik et al., 2002). Fluctuations of  $\alpha$  reflect aerosol size distribution variations. The maximum value of  $\alpha$  (equal to 4) corresponds to molecular extinction. Values near zero (or even negative) correspond to coarse-mode aerosols (sea spray and desert dust) indicating a neutral AOD wavelength dependence, while values of  $\alpha$  above 1.5 indicate significant presence of fine-mode particles (mainly smoke or urban aerosols). However, different aerosol types may be present in the air column at the same time, influencing the observed optical parameters (Chandra et al., 2004) and resulting into intermediate  $\alpha$  values. Remer and Kaufman (1998) showed as well that relative humidity is a determining parameter for the size of aerosol particles. Hygroscopic growth at high relative humidities increases AOD (and reduces  $\alpha$ ), due to the enlargement of soluble particles such as sulphates (Levin et al., 1996).

---

**Aerosol  
characterization in  
N-Africa, NE-Atlantic,  
M. Basin and M. East**S. Basart et al.

---

[Title Page](#)[Abstract](#)[Introduction](#)[Conclusions](#)[References](#)[Tables](#)[Figures](#)[⏪](#)[⏩](#)[◀](#)[▶](#)[Back](#)[Close](#)[Full Screen / Esc](#)[Printer-friendly Version](#)[Interactive Discussion](#)

Therefore,  $\alpha$  alone does not provide unambiguous information on the relative weight of coarse and fine modes because the optical effects of aerosols are essentially bi-modal in nature. In some cases, large fine mode particles can present the same  $\alpha$  than a mixture of coarse mode and small fine mode particles (Gobbi et al., 2007).

5 Several studies have discussed how the spectral variation of  $\alpha$  can provide additional information of the aerosol size distribution (e.g. Kaufman, 1993; Eck et al., 1999; Reid et al. 1999; O'Neill et al, 2003; Schuster et al., 2006; Gobbi et al., 2007). In this sense, Kaufman (1993) pointed-out that negative values of the difference  $\delta\alpha = \alpha(440, 613) - \alpha(613, 1003)$  indicate the dominance of fine mode aerosols, while positive differences reflects the effect of two separate particle modes. Eck et al. (1999) showed how, in the wavelength range of 340–870 nm,  $\alpha$  can increase by a factor of 3–5 as wavelength increases for biomass burning and urban aerosols, while remaining constant or decreasing in the presence of mineral dust. O'Neill et al. (2001) demonstrated that an Ångström exponent-based separation of coarse from fine mode contribution to AOD is feasible in part because of the coarse mode AOD spectral variation being approximately neutral. Schuster et al. (2006) addressed the link between Ångström exponent curvature and the ratio between fine and total aerosol volume. Recently, Gobbi et al. (2007) introduced a straight-forward graphical framework that allows to discriminate different aerosol types based on aerosol spectral measurements by sunphotometers which can be characterized by three independent pieces of information: AOD,  $\alpha$  and the spectral curvature of  $\alpha$  ( $\delta\alpha$ ). Plotting data in this new space allows for inference of aerosol fine mode size and fractional contribution to total AOD.

20 With the possible exception of sea-salt aerosol, mineral dust is globally the most abundant of all aerosol species in the atmosphere (IPCC, 2001). The major sources of contemporary mineral dust production are found on the desert regions of the northern Hemisphere, in the broad “dust belt” that extends from the eastern subtropical Atlantic eastwards through the Sahara Desert to Arabia and southwest Asia, with remarkably little large-scale dust activity outside this region (Prospero et al., 2002). In the present work, we extensively test the new graphical method introduced by Gobbi et al. (2007)

---

**Aerosol  
characterization in  
N-Africa, NE-Atlantic,  
M. Basin and M. East**S. Basart et al.

---

[Title Page](#)[Abstract](#)[Introduction](#)[Conclusions](#)[References](#)[Tables](#)[Figures](#)[⏪](#)[⏩](#)[◀](#)[▶](#)[Back](#)[Close](#)[Full Screen / Esc](#)[Printer-friendly Version](#)[Interactive Discussion](#)

in order to analyze and quantify the contribution of mineral dust to the total aerosol load in Northern Africa, Northeastern Atlantic, Mediterranean Basin and Middle East. Other aerosol types also dominate the atmospheric aerosol load in this region: maritime aerosol, continuously formed over the Mediterranean Sea, the Persian Gulf or the North Atlantic Ocean; fine pollution aerosol (in white and green in Fig. 1) mainly originating from urban and industrial areas of Continental and Eastern Europe, Middle East and along the Nile River; as well as, important contributions of biomass burning (in red in Fig. 1) generated in Africa mainly in winter.

This work provides a thorough overview of the aerosols present into our study region and how the aerosol properties are influenced by long-range transport and local sources. Data and methods are described in Sects. 2 and 3. Results are presented in Sect. 4 where we discuss about the main transport paths of desert dust from source areas and their seasonal behaviour, as well as, the variation of its optical properties through the year in each region of the study area.

## 2 Measurement data

Aerosol optical properties in the entire atmospheric column are routinely observed within the AERONET (AERosol ROBotic NETwork, Holben et al., 1998) program. This is a federation of ground-based remote sensing aerosol networks established by NASA and LOA-PHOTONS (CNRS) and is greatly expanded by collaborators from national agencies, institutes, universities, individual scientists, and partners. The network consists of more than 500 identical globally distributed sun and sky-scanning automated radiometers. The standardized network procedures of instrument maintenance, calibration, cloud screening, and data processing allow for quantitative comparison of the aerosol data obtained at different times and locations (Holben et al., 1998; Smirnov et al., 2000).

These instruments can only retrieve data during daytime, because they rely on extinction measurements of the direct and scattered solar radiation, usually at seven

---

**Aerosol  
characterization in  
N-Africa, NE-Atlantic,  
M. Basin and M. East**S. Basart et al.

---

[Title Page](#)[Abstract](#)[Introduction](#)[Conclusions](#)[References](#)[Tables](#)[Figures](#)[⏪](#)[⏩](#)[◀](#)[▶](#)[Back](#)[Close](#)[Full Screen / Esc](#)[Printer-friendly Version](#)[Interactive Discussion](#)

spectral bands (340, 380, 440, 500, 675, 870 and 1020 nm plus a 940 nm water vapour band). The instrument is out of operation for some weeks while necessary yearly calibration is carried out. Consequently the data coverage in a given station is typically limited to 100–250 days per year. The typical uncertainty in the AOD measured by AERONET instruments ranges from 0.01 to 0.02 and is spectrally dependent with higher errors in the UV spectral range (Holben et al., 1998; Dubovik et al., 2000). These data are provided in three categories: (1) raw (level 1.0), (2) cloud-screened (level 1.5) following the methodology described by Smirnov et al. (2000), and (3) cloud-screened and quality-assured (level 2.0). However, it is worth mentioning that some cases of variable aerosol plumes (like intense Saharan dust outbreaks in regions near to the desert dust sources) could be screened by the cloud-screening algorithm, and conversely, stable uniform clouds might pass the algorithm thresholds and be identified as cloud free (Smirnov et al., 2000).

In the present work, quality-assured direct-sun data in the 440–870 nm wavelength range is used since these channels are highly accurate and they are available in most AERONET instruments. In order to achieve a good temporal coverage, only stations which provided data covering at least the 12 months of the yearly cycle within the 1994–2007 period were chosen. Table 1 and Fig. 2 report the location of the 39 selected AERONET sites. Table 1 lists additional information including type of site, observation periods and percentage of cloud screened data.

### 3 Aerosol classification

In this study we discriminate the fraction of AOD due to large mineral particles from other aerosol types, based on the graphical framework (Fig. 3) introduced in Gobbi et al. (2007) which allows to: (1) infer aerosol fine mode size and fractional contribution to total AOD; and (2) separate AOD increases due to fine-mode aerosol humidification from AOD increases due to the increase in coarse particles. The method relies on the combined analysis of  $\alpha$  derived for the wavelength pairs of 440–675 nm and

675–870 nm and its spectral curvature, represented by  $\delta\alpha = \alpha(440, 675) - \alpha(675, 870)$ . For the definition of these coordinates ( $\delta\alpha$  vs.  $\alpha$  space or AdA coordinates), reference points corresponding to bimodal size distributions characterized by a fine mode modal radii ( $R_f$ ; solid black lines in Fig. 3) as well as the ratio of fine mode to total AOD ( $\eta$ ; dashed blue lines in Fig. 3) have been determined on the basis of typical refractive index of urban/industrial aerosol ( $m = 1.4 - 0.001i$ ). The level of indetermination of this classification scheme is of the order of 25% for  $R_f$  and 10% for  $\eta$  for refractive index varying between  $m = 1.33 - 0.0i$  and  $m = 1.53 - 0.003i$ . Within this level of indetermination, the scheme is robust enough to provide an operational classification of the aerosol properties.

In this space, AOD (at 675 nm) is represented by different colours. In order to avoid errors larger than  $\sim 30\%$  in the calculation of  $\delta\alpha$ , only  $AOD > 0.15$  are considered. Both aging and humidification of pollution aerosol, and coarse-particle contamination could decrease  $\alpha$ . However, these processes behave quite differently in the AdA coordinates, as shown in Fig. 3. Coarse particle contamination is associated to concurrent increase in AOD and coarse mode fraction taking place along  $R_f$  curves (bright green and turquoise lines), while hydration leads to a growth in both  $R_f$  and  $\eta$  (brown diamonds and orange circles). In general, growth of AOD along  $R_f$  lines means an increase in coarse particle extinction. If cloud screening is efficient, only dust particles or maritime aerosols can cause AOD growth along  $R_f$  curves.

Recently, O'Neill (2009) showed that these families of contour lines in the AdA space are essentially empirical and discretized illustrations of analytical parabolic forms in the space formed by the continuously differentiable Ångström exponent ( $\alpha$ ) and its spectral derivative ( $\alpha'$ ). As shown in O'Neill et al. (2003), these variables permits the spectral discrimination of coarse and fine mode optical depth from the spectral shape of AOD by means an spectral algorithm (O'Neill et al., 2001). Thus, both methods are comparable.

---

## Aerosol characterization in N-Africa, NE-Atlantic, M. Basin and M. East

S. Basart et al.

---

Title Page

Abstract

Introduction

Conclusions

References

Tables

Figures

⏪

⏩

◀

▶

Back

Close

Full Screen / Esc

Printer-friendly Version

Interactive Discussion

## 4 Results and discussion

The classification scheme is applied to the 39 AERONET stations considered in this study. Results for fifteen representative locations are reported in Fig. 4 (BAN, ILO, CVR, SAA, IZO, BLI, ARE, ORI, AVI, ROM, THE, LAM, ZIO, MUS and HMM). Seasonal average behaviour is represented in Figs. 5, 6 and 7. Figure 5 includes the mean seasonal AOD,  $\alpha$  and  $\delta\alpha$  for all available measurements with AOD>0.15. Figures 6 and 7 refer to the coarse-particle fraction of the data which includes all data with AOD>0.15 and  $\alpha<0.75$ . As we show along the present section, pure coarse aerosols in the AdA space are always observed in the region  $\alpha<0.75$  in which the fine mode contributions are always <40%. Figure 6 shows the seasonal fraction of the number of coarse mode measurements (with AOD>0.15 and  $\alpha<0.75$ ) with respect to total number of measurements (with AOD>0.15). Figure 7 depicts the mean seasonal contribution to AOD, and  $\alpha$  and  $\delta\alpha$  average of the coarse mode data (with AOD>0.15 and  $\alpha<0.75$ ). As shown in the literature (e.g. Kaufman, 1993), strong negative values of  $\delta\alpha$  (between -0.5 and -0.2) indicate dominance of fine mode aerosols. We have found that under the dominance of coarse mode aerosols, such as desert dust,  $\delta\alpha$  can be negative or slightly positive (between -0.3 and 0.1). Therefore,  $\delta\alpha<0$  values can be related to the presence of a single mode fraction, independently whether it corresponds to fine or to coarse aerosols.

### 4.1 Sahara-Sahel

There are relatively few measurements at Sahelian sites (AGO, BAN, CIN, DAK, OUA, DJO, and ILO) during summer when maximum rainfall and cloud cover occur. A larger number of measurements are observed in the winter or dry season. These stations located southward of Saharan sources show large variations of AOD and high extinctions (~85% of the AOD values are above 0.15 with AOD maxima >4);  $\alpha$  is almost inversely-proportional to AOD, and  $\delta\alpha$  is negative or slightly positive (ranging between -0.3 and 0.1, e.g. BAN in Fig. 4) which indicates that AOD increases are often related

Title Page

Abstract

Introduction

Conclusions

References

Tables

Figures

⏪

⏩

◀

▶

Back

Close

Full Screen / Esc

Printer-friendly Version

Interactive Discussion

to an increase in particle size due to desert dust outbreaks or local dust resuspension. High extinction values ( $AOD > 1$ ) are related to large particles with  $\alpha < 0.3$  and  $\delta\alpha < 0$  that corresponds to  $\eta < 40\%$  and  $R_f \sim 0.3 \mu\text{m}$  which are assumed to be typical of pure desert dust conditions.

As shown in Fig. 6, the proportion of large particles ( $AOD > 0.15$  and  $\alpha < 0.75$ ) is high during the whole year ( $> 50\%$ ), especially in spring (when coarse aerosols represent more than 85% of the data) and summer. Dust transport downwind from source regions vary seasonally. This transport is driven by the latitudinal shift of the Intertropical Front which corresponds to the convergence zone between the northern winds, called the Harmattan, and the monsoon winds coming from the South. From late February to early May the Harmattan wind index is maximum (Sultan et al., 2005). Notice that DJO and ILO show the highest frequency of coarse fractions in spring (Fig. 6).

On the other hand, these stations clearly detected a second aerosol type (i.e. see ILO in Fig. 4) contributing to the turbidity ( $AOD$  up to 1.5) with high  $\alpha$  values ( $\sim 1.5$ ) and negative  $\delta\alpha$  ( $< -0.2$ ) that corresponds to  $\eta \sim 70\%$  and  $R_f \sim 0.13 \mu\text{m}$ . As shown in Fig. 5, ILO and DJO stations present larger contributions of fine aerosols (especially in late autumn-winter) than the rest of sites in this region. This is due to the well-known presence of fine biomass burning aerosols emanating from the sub-Sahel zone (Ogunjobi et al., 2008). The Savannah vegetation is characteristic of the Sudanian zone and fire activities are important during winter. During this season, the interaction of mineral dust and biomass burning aerosols is at its maximum over the region. Thus, all sites present a mixed region associated to  $R_f$  constant curves ( $\sim 0.15 \mu\text{m}$ ) and  $\eta$  between 40 and 70% (see BAN and ILO in Fig. 4). Furthermore, as shown in Fig. 5, all sites present the lowest  $AOD$  values in summer and autumn (coinciding with maximum rainfall and cloud cover). Particularly in ILO and DJO, we observe a decrease in  $\alpha$  values and an increase of  $\delta\alpha$  values ( $\sim 0.10$ ) which indicates the interaction of two separate particle modes. This is due to the presence of fine aerosols from anthropogenic activities in the Nigerian coast.

At higher latitudes, DAH and SAA present relatively few measurements during winter,

## Aerosol characterization in N-Africa, NE-Atlantic, M. Basin and M. East

S. Basart et al.

Title Page

Abstract

Introduction

Conclusions

References

Tables

Figures

⏪

⏩

◀

▶

Back

Close

Full Screen / Esc

Printer-friendly Version

Interactive Discussion

---

**Aerosol  
characterization in  
N-Africa, NE-Atlantic,  
M. Basin and M. East**S. Basart et al.

---

[Title Page](#)[Abstract](#)[Introduction](#)[Conclusions](#)[References](#)[Tables](#)[Figures](#)[⏪](#)[⏩](#)[◀](#)[▶](#)[Back](#)[Close](#)[Full Screen / Esc](#)[Printer-friendly Version](#)[Interactive Discussion](#)

the period of maximum rainfall and cloud cover. They show an important coarse fraction during the whole year (Fig. 6) which is associated to large mineral particles with  $\alpha < 0.6$  and  $\delta\alpha$  slightly negative that corresponds to  $\eta < 50\%$  and AOD maxima  $< 2$  (Fig. 4). As shown in Fig. 6, maximum dust contributions are observed in summertime when the Intertropical Front is found in its northernmost position.

In addition to large mineral particles, SAA (Fig. 4) presents a small fraction of fine aerosols ( $\alpha \sim 1.4$  and  $\delta\alpha \sim -0.5$ ) related to low AODs ( $< 0.2$ ) which corresponds to  $\eta \sim 70\%$  and  $R_f \sim 0.13 \mu\text{m}$  associated to pollution aerosols from local and regional activities. Thus, SAA shows positive  $\delta\alpha$  values (especially in winter) due to the presence of different aerosol modes (e.g. maritime, desert dust and fine pollution aerosols) except in summertime (Fig. 5) when enhanced Saharan dust activity and favourable transport conditions to this area (Middleton and Goudie, 2001) are detected.

## 4.2 Northeastern Atlantic

CVR is located approximately 600 km NW of DAK, in the outflow of Saharan dust from West Africa. In spite of its coastal location CVR (Fig. 4) presents a similar behaviour to the continental station DAK, characterized by a large coarse fraction (Fig. 6) associated to  $\eta < 50\%$  and AOD maxima  $< 3$ . High aerosol loading from spring to autumn (Fig. 5) associated to low  $\alpha$  values and high extinctions indicates that mineral dust dominates the aerosol regime, due to frequent Saharan dust outbreaks. The situation is more complex in wintertime when the aerosol load is lower. In this period, the contribution of sea salt and small particles is significant. As shown in Fig. 4, small particles associated to a  $\eta \sim 70\%$  grows to coarse fractions along  $R_f$  constant curves ( $\sim 0.15 \mu\text{m}$ ). Chemical analysis from samples taken at ground level, and air mass trajectory analysis (Chiapello et al., 1999) already suggested the presence of sulfates transported from urban and industrial regions in southern Europe and/or northwestern Africa, and biomass burning from Savannah fires, as well as, the contribution of local anthropogenic sources.

Roughly 100 km west of the Moroccan coast, in the Canary Islands, we find the SCO (at sea level) and IZO (2370 m a.s.l.) sites. Here quasi-permanent subsidence condi-

---

**Aerosol  
characterization in  
N-Africa, NE-Atlantic,  
M. Basin and M. East**S. Basart et al.

---

[Title Page](#)[Abstract](#)[Introduction](#)[Conclusions](#)[References](#)[Tables](#)[Figures](#)[⏪](#)[⏩](#)[◀](#)[▶](#)[Back](#)[Close](#)[Full Screen / Esc](#)[Printer-friendly Version](#)[Interactive Discussion](#)

tions in the free troposphere together with frequent trade winds flow in the lowest troposphere result in a strong and stable temperature inversion (located at 1400 m a.s.l. in average) that separates a dry free troposphere from a relatively fresh and humid oceanic boundary layer (Torres et al., 2002). The proximity to the Sahara desert and the regional atmospheric circulation exert a decisive influence on the dust climatology of this region (Viana et al., 2002; Querol et al., 2004; Alonso-Pérez et al., 2007). Although these sites are situated very close to each other, they present a very different behaviour (SCO is located at ~50 m sea level within the oceanic boundary layer, whereas IZO is located at ~2370 m a.s.l, normally under free troposphere conditions).

Thus, the background conditions situation at IZO are associated to low AOD values (~85% of its AOD values are under 0.15). As shown in Fig. 4, AODs above 0.15 are associated to large particles with  $\alpha < 0.25$  and  $\delta\alpha \sim 0$  that correspond to  $\eta < 30\%$  (Fig. 4) which are the same values observed at sub-Saharan sites. In winter,  $\text{AOD} > 0.15$  represents <1% of data recorded in this season, while in summer  $\text{AOD} > 0.15$  represents ~50%. This shows an enhanced of Saharan dust transport at this site during summer, in agreement with Prospero et al. (1995).

SCO is located in the city centre of Santa Cruz de Tenerife in the vicinity of the city harbour. This site presents a large coarse fraction associated to  $\eta < 70\%$  and AOD maxima <1.5. High aerosol loading from spring to autumn (Fig. 5) associated to low  $\alpha$  values and high extinctions indicates that mineral dust dominates the aerosol regime, due to frequent Saharan dust outbreaks. The predominance of the trade winds (NE) in the oceanic boundary layer plays a key role in the atmospheric dynamics of this site. It favours the dispersion of pollutants from local urban and industrial activities over the ocean together with the occasional transport of European polluted air masses to this region (Viana et al., 2002). Consequently, the proportion of fine anthropogenic aerosols at SCO is lower than those in regions with similar urban and industrial development in continental environments (Rodríguez and Guerra, 2001; Rodríguez et al., 2008). In general, this fine fraction of pollution aerosols appears well-mixed with coarse mode aerosols like maritime particles (~50% of its  $\text{AOD} > 0.15$  are associated to  $\delta\alpha > 0$ ). Thus,

as shown in Fig. 6, the coarse fraction of this urban site remains very high all year long.

Long-range dust transport above the trade wind inversion layer at IZO is observed from early summer to early-autumn. Low level dust intrusions are detected at SCO mainly in winter (from January to March) and secondary in autumn, in agreement with the previous studies in this North Atlantic region (e.g. Torres et al., 2002; Viana et al., 2002; Alonso-Pérez et al., 2007).

At higher latitudes, we find the Iberian Peninsula. The origin of the air masses arriving to this region is driven by the Azores high pressure system which intensifies during the warm season inducing very weak pressure gradient conditions all over the region (Martin-Vide, 1984). This favours the development of local thermal circulations, such as coastal and mountain breezes. EVO, ROC, ARE, GRA and PAL sites in the Iberian Peninsula show a frequent background situation associated to low AOD values ( $\sim 70\%$  of its AOD values are lower than 0.15). High extinctions ( $AOD > 1$ ) are associated to large particles with  $\alpha < 0.6$  and  $\delta\alpha \sim 0$  that correspond to  $\eta < 30\%$  with a marked South-to-North gradient with AODs maxima  $< 2$  in ARE (Fig. 4) and ROC and  $< 1$  in PAL. These large particles are linked to frequent African dust plumes affecting this area mainly in early-spring and summer (Rodríguez et al., 2001; Silva et al., 2003; Querol et al., 2004; Toledano et al., 2007).

All these sites show a second cluster (see ARE in Fig. 4) associated to  $\alpha > 1.5$  and  $\delta\alpha < -0.2$ . These values correspond to  $\eta \sim 80\%$  and  $R_f \sim 0.13 \mu\text{m}$  related to polluted and continental air masses (Querol et al., 2004; Toledano et al., 2007). In fact, local pollution episodes (mainly in late autumn and winter) as well as emissions from Central and Eastern Europe (Querol et al., 2004) are potential sources of fine aerosol in this region. The one-mode fine aerosol ( $\delta\alpha < 0.1$ ) observed at ARE throughout the year might be caused by its proximity to a huge industrial area (Toledano et al., 2007).

In summertime, under high isolation and low humidity conditions, fine biomass burning aerosols from fires in Iberian Peninsula and Southern France (Belo, 2004) can be detected. AODs during these pollution events ( $0.15 < AOD < 0.7$ ) are lower than those recorded during African dust outbreaks but clearly higher than those observed during

**Aerosol  
characterization in  
N-Africa, NE-Atlantic,  
M. Basin and M. East**

S. Basart et al.

Title Page

Abstract

Introduction

Conclusions

References

Tables

Figures

⏪

⏩

◀

▶

Back

Close

Full Screen / Esc

Printer-friendly Version

Interactive Discussion

background Atlantic advection conditions. This fine particle cluster grows following the constant  $R_f$  curves ( $\sim 0.13 \mu\text{m}$ ) due to the presence of coarse particles (likely maritime aerosols). Additionally, in winter (under stagnant conditions), a growth of AOD along constant  $\eta$  lines ( $\sim 85\%$ ), linked to both coagulation-aging and hydration, is observed.

Although African dust outbreaks over the Iberian Peninsula can occur throughout the year, its contribution to AOD is more important in spring (Fig. 6). In this season, coarse particles normally appear well-mixed with other types of small particles as indicated by positive  $\delta\alpha$  values ( $\sim 0.20$ ). Additionally, it is remarkable the seasonal differences (Fig. 7) between the sites located in south-western part of the Peninsula (ARE, ROC and EVO) and south-eastern (GRA) indicating different transport patterns at both areas.

### 4.3 Mediterranean Basin

The Mediterranean basin is characterized by cold winters and hot summers. The stable anticyclonic weather conditions permits continuous measurements over long periods, especially in summer.

#### 4.3.1 Western Mediterranean

The stations located in the Northwestern Mediterranean coast are close to numerous industrial and urban sources of primary pollutants. AVI (Fig. 4), TUL, CAR, VIL and BCN sites present an important fine particle cluster in the AdA space ( $\alpha > 1.6$  and  $\delta\alpha < -0.3$ ) associated to  $\eta \sim 80\%$  and  $R_f \sim 0.12 \mu\text{m}$ . In fact, more than 70% of their datasets are associated to this fine particle cluster (Fig. 6) which correspond to moderate extinctions ( $\text{AOD} < 0.7$ ). AOD growth is linked to both coagulation-aging and hydration increase of  $R_f$ . At the same time coarse particles, likely maritime aerosols, superimpose their signal onto this fine mode. As shown in Fig. 4, a concurrent increase in AOD and coarse mode fraction along the  $R_f$  curves ( $\sim 0.12 \mu\text{m}$ ) is observed. Conversely, highest extinctions ( $\text{AOD maxima} > 1$ ) are related to large particles ( $\alpha < 0.7$ ) that

Title Page

Abstract

Introduction

Conclusions

References

Tables

Figures

⏪

⏩

◀

▶

Back

Close

Full Screen / Esc

Printer-friendly Version

Interactive Discussion

---

**Aerosol  
characterization in  
N-Africa, NE-Atlantic,  
M. Basin and M. East**S. Basart et al.

---

[Title Page](#)[Abstract](#)[Introduction](#)[Conclusions](#)[References](#)[Tables](#)[Figures](#)[⏪](#)[⏩](#)[◀](#)[▶](#)[Back](#)[Close](#)[Full Screen / Esc](#)[Printer-friendly Version](#)[Interactive Discussion](#)

corresponds to  $\eta < 40\%$ . This coarse particle cluster is associated to large dust aerosols from North African deserts. As shown in Fig. 7, coarse fraction exhibits positive  $\delta\alpha$  values throughout the year which indicates the presence of small particles mixed with this coarse mode. The Northwestern Mediterranean coast is characterized by a high frequency of breeze-type circulations, which are intensified by topography. Under weak pressure gradients, coastal and nearby mountain breeze regime predominates favouring the development of polluted atmospheric layers at several heights (Pérez et al., 2004; Jimenez et al., 2006). Thus, Saharan dust is found at high altitudes while, fine pollution aerosols are concentrated at lower altitudes (e.g. Pérez et al., 2004). North African highs, located at surface level, and Atlantic depressions west of Portugal, favour air mass transport at low levels from the Western Sahara, Mauritania and the Sahel to the Northwestern Mediterranean (Moulin et al., 1998; Rodríguez et al., 2001; Escudero et al., 2005). These meteorological conditions are typically associated with the presence of rain resulting in the well-known “red rains” (Ávila et al., 1998). Thus, most of the Saharan intrusions during these rainy periods have not been recorded into our dataset because AERONET instruments are not operative during rainy events.

#### 4.3.2 Central Mediterranean

At southern latitudes, ORI, on the west coast of Sardinia, and BLI, in the Algerian coast, exhibit high extinctions ( $AOD > 0.7$ ) in the coarse fraction. This is caused by frequent North African dust advections. Both sites (included in Fig. 4) present highest extinctions ( $AOD > 1$ ) in the coarse mode ( $\alpha < 0.4$  and  $\delta\alpha \sim 0$ ) that corresponds to  $\eta < 30\%$ . Additionally to this coarse cluster, we detect in the AdA space a small fraction of fine aerosols ( $\alpha \sim 1.6$  and  $\delta\alpha \sim -0.5$ ) from local anthropogenic sources and European pollution which is most important at the ORI site. This fine cluster is related to low extinctions ( $AOD < 0.3$ ) and  $\eta > 70\%$ . A simultaneous growth of AOD and coarse fraction (indicated by a decrease of  $\alpha$ ) along constant  $R_f$  curves is associated to cloud contamination. At the same time, coarse particles (likely dust) superimpose their signal onto this fine mode particles.

---

**Aerosol  
characterization in  
N-Africa, NE-Atlantic,  
M. Basin and M. East**

---

S. Basart et al.

---

[Title Page](#)[Abstract](#)[Introduction](#)[Conclusions](#)[References](#)[Tables](#)[Figures](#)[⏪](#)[⏩](#)[◀](#)[▶](#)[Back](#)[Close](#)[Full Screen / Esc](#)[Printer-friendly Version](#)[Interactive Discussion](#)

As shown in Fig. 6, the coarse fraction is most important in BLI than ORI during all year due to its proximity to African sources. Maximum contributions in spring and summer and minima in winter are observed, coinciding with the maximum and minimum incidence of Saharan dust transport, respectively, in this part of the Mediterranean basin (Barnaba and Gobbi, 2004). Note the similarities in Figs. 5 and 6 between BLI and GRA (in the Iberian Peninsula) indicating common African dust sources and pathways at both locations.

At about 130 km east from the Tunisian coast, LAM (Fig. 4) shows an important cluster in the coarse mode in the AdA space ( $\alpha < 0.5$  and  $\delta\alpha \sim 0$ ) associated to frequent Saharan dust outbreaks to this site (Pace et al., 2006) that corresponds to  $\eta < 50\%$ . This coarse contribution is high throughout the year (Fig. 6) and high extinctions ( $AOD > 1$  and ranging up to 2.5) are related to almost pure desert dust ( $\eta < 30\%$ ,  $\alpha < 0.3$  and  $\delta\alpha \sim 0$ ) as observed in Sub-Saharan sites. Moreover, a second aerosol type (Fig. 4) with  $AOD < 0.4$  and  $\alpha \sim 1.8$  that corresponds to  $\eta \sim 90\%$  and  $R_f \sim 0.14 \mu\text{m}$  is observed. A growth of AOD and coarse fraction is found along the constant  $R_f$  curves due to the presence of coarse particles. In summertime, when wet removal is practically absent and photochemical reactions are favoured, the contribution of small pollution particles is maximum (Fig. 6). They are related to long-range transport of urban and industrial aerosols from Western, Central and Eastern Europe as well as from biomass burning (Pace et al., 2006). In winter,  $AOD > 0.15$  represents  $< 7\%$  of data and it is associated to dust events (Figs. 5 and 6). In this season, the high contribution of aerosols associated to lower AOD values ( $< 0.15$ ) indicates contribution of maritime aerosols and a minimum incidence of long range transport.

Further north, in the Italian Peninsula, ROM (Fig. 4) and LEC sites show an important fine cluster in the AdA space ( $\alpha > 1.8$  and  $\delta\alpha \sim -0.4$ ) that corresponds to  $\eta \sim 80\%$  and  $R_f \sim 0.12 \mu\text{m}$ . The fine mode at ROM is mainly due to secondary particles of local origin, and long range transport is a minor component (Gobbi et al., 2004). On the contrary, LEC presents a more important contribution of fine pollution aerosols transported from Central and Eastern Europe (Lelieveld et al., 2002), and from the Atlantic Ocean (De

---

**Aerosol  
characterization in  
N-Africa, NE-Atlantic,  
M. Basin and M. East**S. Basart et al.

---

[Title Page](#)[Abstract](#)[Introduction](#)[Conclusions](#)[References](#)[Tables](#)[Figures](#)[⏪](#)[⏩](#)[◀](#)[▶](#)[Back](#)[Close](#)[Full Screen / Esc](#)[Printer-friendly Version](#)[Interactive Discussion](#)

Tomasi and Perrone, 2003). LEC is also affected by fine particles originated by frequent summertime forest fires (Perrone et al., 2005). At both sites, a simultaneous growth of AOD and coarse fraction (indicated by a decrease of  $\alpha$ ) along constant  $R_f$  curves in the AdA space is associated to the presence of coarse particles (likely dust). In addition, in ROM (Fig. 4), the extension of fine pollution particles to higher AOD occurs perpendicularly to the black line. This is due to the coexistence of mineral dust and fine pollution aerosols. Additionally, both sites, are impacted by Saharan dust with AOD>0.4 (with AOD maxima of 1.5) and  $\alpha<0.75$  that corresponds to  $\eta<30\%$ . This coarse cluster is more important at LEC than at ROM (Fig. 6) and it usually appears well-mixed with other small particles (Fig. 7). Thus, ROM and LEC present different seasonal features (Figs. 6 and 7). The high contribution of large size aerosols at LEC in winter (Figs. 5 and 6) is due to the lower contribution of long-range transported fine particles and a higher weather instability that does not favour the accumulation of fine particles. From spring to autumn, a decrease of  $\alpha$  values (Fig. 5) is associated to an increase of the frequency of long-range transport of Saharan dust to southern and central Italy (Pappalardo et al., 2003; Barnaba and Gobbi, 2004; Gobbi et al., 2004).

### 4.3.3 Eastern Mediterranean

In the Central-Eastern Mediterranean large particles are quasi inexistent at THE (Fig. 6). This site is characterized by rather heavy pollution being strongly influenced by regional (Central and Eastern Europe) and local urban and industrial sources as well as by biomass burning that may also contribute sporadically from areas at the northern coast of the Black Sea (Gerasopoulos et al., 2003). As shown in Fig. 4, high extinctions (AOD>0.7) mainly clustering in the fine mode ( $\alpha\sim 1.8$  and  $\delta\alpha\sim -0.3$ ) that corresponds to  $\eta\sim 85\%$  and  $R_f\sim 0.13\mu\text{m}$ . This fine polluted cluster presents a growing AOD linked to both coagulation-aging (along constant  $\eta\sim 85\%$ ) and hydration-type increase along  $R_f$  constant. Occasional events of long-range transport of desert dust are observed only in summer (Fig. 6) and commonly appear mixed with fine pollution aerosols (Fig. 4). These desert dust events are associated to AODs between 0.7 and

1 as also suggested in Balis et al. (2006).

In the Eastern Mediterranean, CRE, ERD, ZIO (Fig. 4), SED and CAI sites present high extinctions ( $AOD > 1$ ) associated to clustering in the coarse mode ( $\alpha < 0.75$ ) in the AdA space. They are related to large mineral aerosols originated in desert dust source regions such as Anatolian plateau, Saharan and Negev deserts (Andreae et al., 2002; Kubilay et al., 2003; Derimian et al., 2006) corresponding to  $\eta < 40\%$ . As shown in Figs. 5, 6 and 7, maximum contribution of the coarse particles, associated to high extinctions, is observed in spring in this area. During this season, long-range Saharan dust transport and uplifted dust particles from surrounding deserts are very important (Kubilay et al., 2000, 2003; Barnaba and Gobbi, 2004).

The aerosol climatology of CRE site is strongly determined by the maritime environment with high concentrations of sea-salt aerosols ( $> 65\%$  of its AOD is  $< 0.15$ ) which constitute the background conditions. The CRE data shows high AOD ( $> 0.7$ ), mainly clustering in the coarse mode ( $\alpha < 0.6$  and  $\delta\alpha \sim 0$ ) that corresponds to  $\eta < 30\%$ . These large particles are related to long-range transport from Sahara, and, in minor degree, from source regions in the eastern part of Mediterranean basin (such as Anatolian plateau, Saharan and Negev deserts) and Middle East (Dayan et al., 1991; Kubilay et al., 2000; Barnaba and Gobbi, 2004; Fotiadi et al., 2006). As shown in Figs. 5 and 6, maximum contributions of this coarse mode are observed in winter and spring. In winter,  $AOD > 0.15$  represents  $< 20\%$  of data and it is associated to dust events (Figs. 5 and 6). In this season, high contribution of aerosols associated to lower AOD values ( $< 0.15$ ) is a consequence of the background situation dominated by the presence of maritime aerosols (Fotiadi et al., 2006). In spring, a decrease of  $\delta\alpha$  values ( $\sim 0$ ) in the coarse mode with respect to the rest of the year (Fig. 7) indicates an increase of long-range dust transport to this area. Contributions from urban-industrial aerosol intrusions into the region from the Eastern Europe, Balkan area, and Anatolia maximize in summer (Figs. 5 and 6). This fine mode ( $\alpha > 1.5$  and  $\delta\alpha \sim -0.2$ ) is associated to low AODs ( $< 0.4$ ) and corresponds to  $\eta > 70\%$ . The growth to higher AODs and coarse fractions occurs perpendicularly to the constant  $R_f$  line due to the coexistence of coarse

**Aerosol  
characterization in  
N-Africa, NE-Atlantic,  
M. Basin and M. East**

S. Basart et al.

Title Page

Abstract

Introduction

Conclusions

References

Tables

Figures

⏪

⏩

◀

▶

Back

Close

Full Screen / Esc

Printer-friendly Version

Interactive Discussion

aerosols (likely maritime) and small pollution particles. Therefore, is a common situation that they appear well-mixed as indicated by positives values of  $\delta\alpha$  throughout the year (Fig. 5).

A second cluster in the fine mode region ( $\alpha\sim 1.6$  and  $\delta\alpha\sim -0.3$ ), that corresponds to  $\eta\sim 70\%$  and  $R_f\sim 0.14\ \mu\text{m}$ , is observed. This fine mode is associated to pollution particles and it is especially remarkable at sites on the coasts of Turkey and Israel such as ERD and ZIO (Fig. 6), where the urban-industrial local emissions are significant. Most of the long-range transported aerosol in this region is attributed to Central and Eastern Europe, especially along the Israeli coast (Sciare et al., 2003; Fotiadi et al., 2006), as well as to Southern Russia (Andreae et al., 2002; Derimian et al., 2006) with additional contributions from marine biogenic activities and forest fires in the region. This fine cluster presents an increase in AOD and coarse mode fraction along the constants  $R_f$  curves (see ZIO in Fig. 4), moreover, the growth to higher AODs also occurs perpendicularly to the constant  $R_f$  line (see ZIO in Fig. 4). This is due to the coexistence of mineral dust and fine pollution aerosols. Additionally, in high-pollution locations (such as ZIO and ERD), branching of data along  $\eta$  lines is observed which is associated to coagulation-aging growth. The contribution of small pollution particles is maxima in summer (Fig. 6), when wet removal is practically absent and the accumulation of pollution is favoured.

#### 4.4 Middle East

The sites located in the Arabian Peninsula (MUS, DHA, DHD, BHR, HMM and SVI) provide a relatively large amount of measurements thanks to stable weather conditions in this region. The United Arab Emirates and the Persian Gulf include strong regional desert dust sources of predominately coarse mode-size particles, as well as important fine mode pollution particle sources from petroleum extraction and processing facilities which are located on islands, sea-platforms and coastal regions of the Persian Gulf. Thus, as shown in Fig. 5, the coastal sites in the northeastern part of the United Arab Emirates such as MUS, DHA and DHD, as well as BHR in the Persian Gulf, attain

**Aerosol  
characterization in  
N-Africa, NE-Atlantic,  
M. Basin and M. East**

S. Basart et al.

Title Page

Abstract

Introduction

Conclusions

References

Tables

Figures

⏪

⏩

◀

▶

Back

Close

Full Screen / Esc

Printer-friendly Version

Interactive Discussion



positive  $\delta\alpha$  values during almost all year ( $\sim 0.2$ ) which indicate the coexistence of two particle modes.

For the coastal sites of MUS (Fig. 4), DHA, DHD and BHR, we observe desert dust with AOD maxima of 1.5,  $\alpha < 0.75$  and  $\delta\alpha \geq 0$  that corresponds to  $\eta < 40\%$ . As opposite, small particles from petroleum industry emissions are associated to fine mode ( $\alpha \sim 1.6$  and  $\delta\alpha \sim -0.2$ ) and  $\text{AOD} < 0.7$  corresponding to  $\eta > 70\%$  and  $R_f \sim 0.13 \mu\text{m}$ . The interaction of mineral dust and pollution is strong in these coastal sites. In the AdA space, this mixed region follows  $R_f$  constant curves and is associated to  $\eta$  between 40 and 70% (see MUS in Fig. 4). Additionally, and due to the proximity of these stations to the sea, an increase in AOD is linked to both coagulation-aging and hygroscopic-type increase in  $R_f$ .

Conversely, at the inland desert sites, as HMM (Fig. 4) and SVI, desert dust is the main aerosol the main aerosol constituent, being associated with high AOD ( $> 0.7$  ranging up  $> 2$ ) mainly clustering in the coarse mode ( $\alpha < 0.75$  and  $\delta\alpha$  variable). This cluster corresponds to  $\eta < 50\%$ . HMM ( $\sim 125 \text{ km}$  inland from the Gulf; Fig. 4) shows a contribution of small particles from industrial emissions that corresponds to  $\eta \sim 80\%$  and  $R_f \sim 0.13 \mu\text{m}$ . This transport is consequence of regional sea and land breeze circulations in this area (Eck et al., 2008) which produces occasional increases of fine mode particles from offshore petroleum operations. This fine mode presents a growth of AOD and coarse mode fraction along the constants  $R_f$  curves. Otherwise, SVI is located in the middle of the Arabian Peninsula, near to At Riyadh (the capital of Saudi Arabia and its largest city) and far away from the Persian Gulf or other industrialized areas. SVI presents its highest extinctions ( $\text{AOD} > 1$ ) in the coarse mode region ( $\alpha < 0.75$  and  $\delta\alpha < 0.1$ ) which presents an expanded particle size distribution. It ranges from almost pure coarse-mode dust particles (associated to  $\alpha < 0.3$  and  $\eta < 30\%$ ) to a mixture of coarse particles and regional fine-mode pollution aerosols ( $\eta < 70\%$ ) caused by anthropogenic activities in the region (Kaskaoutis et al., 2007).

As shown in Fig. 6, the contribution of large particles is maximum in spring and summer. In spring, all sites present similar AODs and  $\alpha$  values (Fig. 5). It is associated

---

## Aerosol characterization in N-Africa, NE-Atlantic, M. Basin and M. East

S. Basart et al.

---

Title Page

Abstract

Introduction

Conclusions

References

Tables

Figures

⏪

⏩

◀

▶

Back

Close

Full Screen / Esc

Printer-friendly Version

Interactive Discussion

to maximum desert dust local activity (Smirnov et al., 2002b; Eck et al., 2005; Kim et al., 2007; Kaskaoutis et al., 2007). On the contrary, in summer, MUS, DHA, DHD and HMM show higher AODs than BHR and SVI coinciding with a general increase of  $\alpha$  values (Fig. 5). In this season, the southwest monsoon introduces a northwesterly flow over the Arabian Peninsula bringing extremely dry and dust-loaded air from the Iraq and southern Iran deserts (Liu et al., 2000). In addition to long range transport, regional sea-land breeze circulations cause both, a regional transport of polluted and humid air masses from the Persian Gulf to inland regions, and a dust transport from these regions towards the coast and the Gulf (Eck et al., 2008) favouring a mixing of desert dust and fine pollution aerosols.

## 5 Summary and conclusions

In the present work, we have provided an aerosol characterization (mainly focusing on the contribution of mineral particles) based on direct-sun observations of 39 AERONET stations which include at least an annual cycle within the 1994–2007 period. These stations are located in the region most affected by the presence of Saharan and Arabian desert dust: Northern Africa, Northeastern Atlantic, Mediterranean Basin and Middle East. In addition to large mineral particles, fine pollution aerosols, originated in industrialized countries surrounding the Mediterranean Sea and in the Persian Gulf, and biomass burning aerosols, produced in the Sahel and southern European countries, are expected to dominate the atmospheric aerosol load in this region.

The method used to discriminate different aerosol types, introduced in Gobbi et al. (2007), relies on the combined analysis of the Ångström exponent ( $\alpha$ ) and its spectral curvature, here represented by  $\delta\alpha = \alpha(440, 675) - \alpha(675, 870)$ . Plotting data in these coordinates was shown to allow for inference of aerosol fine mode size ( $R_f$ ) and fractional contribution ( $\eta$ ) to total AOD by means of the inclusion of reference points. It is also possible to separate the AOD increase due to fine-mode aerosol humidification and/or coagulation, from AOD growth due to the increase in coarse particles or cloud

Title Page

Abstract

Introduction

Conclusions

References

Tables

Figures

⏪

⏩

◀

▶

Back

Close

Full Screen / Esc

Printer-friendly Version

Interactive Discussion

contamination.

In Northern Africa, mineral dust is found to be the main aerosol constituent, being associated with coarse mode particles that corresponds to  $\eta < 40\%$ . Highest extinctions (AOD > 4) are related to  $\eta < 30\%$  and  $R_f \sim 0.3 \mu\text{m}$  that we assumed as typical of pure Saharan dust particles. Superimposed to this coarse cluster, small particles associated to fine mode ( $\alpha > 1.5$  and  $\delta\alpha \sim -0.3$ ), that corresponds to  $\eta \sim 70\%$  and  $R_f \sim 0.13 \mu\text{m}$ , are also observed. In southern sites, in the Sahel region, this fine contribution is limited to winter and it is originated by biomass burning, meanwhile, at northern latitudes, the fine cluster is most important and is linked to the local or regional urban-industrial emissions. Frequently, the interaction of large mineral particles and small aerosols results in a well-mixed conditions associated to  $\delta\alpha > 0$ . Northeastern Atlantic sites located in the outflow of Saharan dust from West Africa present similar behaviour to the continental stations located at the same latitudes, characterized by a large mineral dust fraction from spring to autumn.

Southern Europe is dominated by fine anthropogenic aerosol but sporadically is affected by the presence of coarse dust particles. In spite of the Iberian Peninsula sites show a frequent background situation associated to low AOD values ( $< 0.15$ ), high extinctions (AOD > 1) are associated to large particles with  $\alpha < 0.6$  and  $\delta\alpha \sim 0$  that correspond to  $\eta < 30\%$  with a marked South-to-North gradient which are linked to frequent African dust plumes affecting this area mainly in early-spring and summer. Additionally, a second cluster associated to  $\alpha > 1.5$  and  $\delta\alpha < -0.2$  that correspond to  $\eta \sim 80\%$  and  $R_f \sim 0.13 \mu\text{m}$  can be related to polluted and European continental air masses. The highest polluted sites in the central-eastern Mediterranean show measurements clustering in the fine mode ( $\alpha > 1.5$  and  $\delta\alpha \sim -0.3$ ) that corresponds to  $\eta > 70\%$  and  $R_f \sim 0.13 \mu\text{m}$ . In these cases the AOD increase is linked to both coagulation-aging and hydration type increase in  $R_f$ . Furthermore, a North-to-South AOD gradient, related to coarse mode ( $\alpha < 0.75$  and  $\delta\alpha$  variable), that corresponds to  $\eta < 40\%$ , is associated to seasonal dust export. In general, the maximum dust activity appears in spring and summer over the whole Mediterranean Basin. During spring the main aerosol activity takes place in the

**Aerosol  
characterization in  
N-Africa, NE-Atlantic,  
M. Basin and M. East**

S. Basart et al.

Title Page

Abstract

Introduction

Conclusions

References

Tables

Figures

⏪

⏩

◀

▶

Back

Close

Full Screen / Esc

Printer-friendly Version

Interactive Discussion

**Aerosol  
characterization in  
N-Africa, NE-Atlantic,  
M. Basin and M. East**

S. Basart et al.

Title Page

Abstract

Introduction

Conclusions

References

Tables

Figures

⏪

⏩

◀

▶

Back

Close

Full Screen / Esc

Printer-friendly Version

Interactive Discussion

Eastern Mediterranean, where dust is transported by thermal lows. In summer, the maximum of dust activity occurs in the Central Mediterranean. By late summer–early autumn, under the influence of low pressures near the Balearic Islands, the maximum dust activity is found in the Western Mediterranean. In wintertime, the high contribution of aerosols associated to lower AOD values ( $<0.15$ ) indicates significant contributions from maritime aerosols compared to dust. However, some few dust outbreaks can also take place in this season.

In general, desert dust appears well-mixed with other types of particles like fine pollution aerosols. They are associated to  $AOD < 1$ , but in some intense Saharan outbreaks (with  $\delta\alpha \sim 0$ ) can reach AOD values of 2. The long-range transport of these dust particles usually occurs at higher altitudes (above 1500 m a.s.l.), whereas, urban-industrial and maritime aerosols concentrate in lower altitudes.

In the Middle East, all sites show high extinctions ( $AOD < 3$ ) mainly clustering in the coarse mode that corresponds to  $\eta < 50\%$ . These extinctions are lower than those observed in the African sites. In coastal sites of the Persian Gulf, fine-mode aerosols ( $\alpha > 1.6$  and  $\delta\alpha \sim -0.3$ ) largely produced by petroleum industry, are observed. They are associated to  $\eta > 70\%$  and  $R_f \sim 0.13 \mu\text{m}$ . The AOD increase is linked to both coagulation-aging and hydration-type increase  $R_f$  due to very humid conditions in the Gulf. This variability of atmospheric particle types in conjunction with highly variable regional meteorology, results in a high variety of situations in this region: some days are dominated by large particle desert dust, while others by fine pollution particles. However most of the days are characterized by a mixture of these two aerosol types.

Finally, this study confirms the robustness of the method of Gobbi et al. (2007) based on direct-sun measurements (more frequent and accurate than sky measurements) to track and analyze mixtures of pollution aerosol and mineral dust. Thus, we have shown that  $\delta\alpha < 0$  values can be related to the presence of a single mode fraction, independently whether it corresponds to fine or to coarse aerosols.

*Acknowledgements.* This work is the first step of a long way to walk. We wish to acknowledge the AERONET and PHOTONS networks, and to the research groups that contribute to them,

who kindly provided their data. This work was funded by the project CICYT CGL2006-11879 of the Spanish Ministry of Education and Science.

## References

- Alonso-Pérez, S., Cuevas, E., Querol, X., Viana, M., and Guerra, J. C.: Impact of the Saharan dust outbreaks on the ambient levels of total suspended particles (TSP) in the marine boundary layer (MBL) of the Subtropical Eastern North Atlantic Ocean, *Atmos. Environ.*, 41(40), 9468–9480, 2007.
- Andreae, T. W., Andreae, M. O., Ichoku, C., Maenhaut, W., Cafmeyer, J., Karnieli, A., and Orlovsky, L.: Light scattering by dust and anthropogenic aerosol at a remote site in the Negev desert, Israel, *J. Geophys. Res.*, 107(D2), doi:10.1029/2001JD900252, 2002.
- Ångström, A.: On the Atmospheric Transmission of Sun Radiation and on Dust in the Air, *Geogr. Ann.*, 11, 156–166, 1929.
- Ávila, A., Alarcón, M., and Queralt, I.: The chemical composition of dust transported in red rains- Its contribution to the biogeochemical cycle of a holm oak forest in Catalonia (Spain), *Atmos. Environ.*, 32(2), 179–191, 1998.
- Balis, D., Amiridis, V., Kazadzis, S., Papayannis, A., Tsaknakis, G., Tzortzakis, S., Kalivitis, N., Vrekoussis, M., Kanakidou, M., Mihalopoulos, N., Chourdakis, G., Nickovic, S., Pérez, C., Baldasano, J., and Drakakis, M.: Optical characteristics of desert dust over the East Mediterranean during summer: a case study, *Ann. Geophys.*, 24, 807–821, 2006, <http://www.ann-geophys.net/24/807/2006/>.
- Barnaba, F. and Gobbi, G. P.: Aerosol seasonal variability over the Mediterranean region and relative impact of maritime, continental and Saharan dust particles over the basin from MODIS data in the year 2001, *Atmos. Chem. Phys.*, 4, 2367–2391, 2004, <http://www.atmos-chem-phys.net/4/2367/2004/>.
- Belo, N.: Caracterização das propriedades ópticas dos aerossóis à superfície na região de Évora. Departamento de Física, Universidade de Lisboa, Lisboa, 100 pp., 2004.
- Chandra, S., Satheesh, S. K. and Srinivasan, J.: Can the state of mixing of black carbon aerosols explain the mystery of “excess” atmospheric absorption?, *J. Geophys. Res. Lett.*, 31(L19109), doi:10.1029/2004GL020662, 2004.
- Chiappello, I., Bergametti, G., Chatenet, B., Dulac, F., Jankowiak, I., Liousse, C., and Santos

## Aerosol characterization in N-Africa, NE-Atlantic, M. Basin and M. East

S. Basart et al.

Title Page

Abstract

Introduction

Conclusions

References

Tables

Figures

⏪

⏩

◀

▶

Back

Close

Full Screen / Esc

Printer-friendly Version

Interactive Discussion

---

**Aerosol  
characterization in  
N-Africa, NE-Atlantic,  
M. Basin and M. East**S. Basart et al.

---

[Title Page](#)[Abstract](#)[Introduction](#)[Conclusions](#)[References](#)[Tables](#)[Figures](#)[⏪](#)[⏩](#)[◀](#)[▶](#)[Back](#)[Close](#)[Full Screen / Esc](#)[Printer-friendly Version](#)[Interactive Discussion](#)

- Soares, E.: Contribution of the different aerosol species to the aerosol mass load and optical depth over the northeastern tropical Atlantic, *J. Geophys. Res.*, 104(D4), 4025–4035, 1999.
- Dayan, U., Heffter, J., Miller, J., and Gutman, G.: Dust Intrusion Events into the Mediterranean Basin, *Appl. Meteorol.*, 30(8), 1185–1199, 1991.
- 5 De Tomasi, F. and Perrone, M. R.: Lidar measurements of tropospheric water vapor and aerosol profiles over southeastern Italy, *J. Geophys. Res.*, 108, 4286–4297, 2003.
- Derimian, Y., Karnieli, A., Kaufman, Y. J., Andreae, M. O., Andreae, T. W., Dubovik, O., Maenhaut, W., Koren, I., and Holben, B. N.: Dust and pollution aerosols over the Negev desert, Israel: Properties, transport, and radiative effect, *J. Geophys. Res.*, 111(D05205), doi:10.1029/2005JD006549, 2006.
- 10 Dubovik, O., Smirnov, A., Holben, B. N., King, M. D., Kaufman, Y. J., Eck, T. F., and Slutsker, I.: Accuracy assessments of aerosol optical properties retrieved from Aerosol Robotic Network (AERONET) Sun and sky radiance measurements, *J. Geophys. Res.*, 105(D8), 9791–9806, 2000.
- 15 Dubovik, O., Holben, B. N., Eck, T. F., Smirnov, A., Kaufman, Y. J., King, M. D., Tarré, D., and Slutsker, I.: Variability of Absorption and Optical Properties of Key Aerosol Types Observed in Worldwide Locations, *Atmos. Sci.*, 59, 590–608, 2002.
- Eck, T. F., Holben, B. N., Reid, J. S., Dubovik, O., Smirnov, A., O'Neill, N. T., Slutsker, I., and Kinne, S.: Wavelength dependence of optical depth of biomass burning, urban and desert dust aerosols, *J. Geophys. Res.*, 104(D24), 31333–31350, 1999.
- 20 Eck, T. F., Holben, B. N., Dubovik, O., Smirnov, A., Goloub, P., Chen, H. B., Chatenet, B., Gomes, L., Zhang, X. Y., and Tsay, S. C.: Columnar aerosol optical properties at AERONET sites in central eastern Asia and aerosol transport to the tropical mid-Pacific, *J. Geophys. Res.*, 110, D06202, doi:10.1029/2004JD005274, 2005.
- 25 Eck, T. F., Holben, B. N., Reid, J. S., Sinyuk, A., Dubovik, O., Smirnov, A., Giles, D., O'Neill, N. T., Tsay, S. C., and Ji, Q.: Spatial and temporal variability of column-integrated aerosol optical properties in the southern Arabian Gulf and United Arab Emirates in summer, *J. Geophys. Res.*, 113, D01204, doi:10.1029/2007JD008944, 2008.
- Escudero, M., Castillo, S., Querol, X., Avila, A., Alarcón, M., Viana, M. M., Alastuey, A., Cuevas, E., and Rodriguez, S.: Wet and dry African dust episodes over Eastern Spain, *J. Geophys. Res.*, 110, 4731–4746, 2005.
- 30 Fotiadis, A., Drakakis, E., Hatzianastassiou, N., Matsoukas, C., Pavlakis, K. G., Hatzidimitriou, D., Gerasopoulos, E., Mihalopoulos, N., and Vardavas, I.: Aerosol physical and optical prop-

---

**Aerosol  
characterization in  
N-Africa, NE-Atlantic,  
M. Basin and M. East**S. Basart et al.

---

[Title Page](#)[Abstract](#)[Introduction](#)[Conclusions](#)[References](#)[Tables](#)[Figures](#)[⏪](#)[⏩](#)[◀](#)[▶](#)[Back](#)[Close](#)[Full Screen / Esc](#)[Printer-friendly Version](#)[Interactive Discussion](#)

erties in the Eastern Mediterranean Basin, Crete, from Aerosol Robotic Network Data, Atmos. Chem. Phys., 6, 7791–7834, 2006, <http://www.atmos-chem-phys.net/6/7791/2006/>.

Gerasopoulos, E., Andreae, M. O., Zerefos, C. S., Andreae, T. W., Balis, D., Formenti, P., Merlet, P., Amiridis, V., and Papastefanou, C.: Climatological aspects of aerosol optical properties in Northern Greece, Atmos. Chem. Phys., 3, 2059–2099, 2003, <http://www.atmos-chem-phys.net/3/2059/2003/>.

Gobbi, G. P., Barnaba, F., and Ammannato, L.: The vertical distribution of aerosols, Saharan dust and cirrus clouds in Rome (Italy) in the year 2001, Atmos. Chem. Phys., 4, 351–359, 2004, <http://www.atmos-chem-phys.net/4/351/2004/>.

Gobbi, G. P., Kaufman, Y. J., Koren, I., and Eck, T. F.: Classification of aerosol properties derived from AERONET direct sun data, Atmos. Chem. Phys., 7, 453–458, 2007, <http://www.atmos-chem-phys.net/7/453/2007/>.

Holben, B. N., Eck, T. F., Slutsker, I., Tarré, D., Buis, J. P., Setzer, A., Vermote, E., Reagan, J., Kaufman, Y., Nakajima, T., Lavenue, F., Jankowiak, I., and Smirnov, A.: AERONET: A Federated Instrument Network and Data Archive for Aerosol Characterization, Remote Sens. Environ., 66, 1–16, 1998.

Holben, B. N., Tanre, D., Smirnov, A., Eck, T. F., Slutsker, I., Abuhassan, N., Newcomb, W. W., Schafer, J., Chatenet, B., Lavenue, F., Kaufman, Y. J., Castle, J. V., Setzer, A., Markham, B., Clark, D., Frouin, R., Halthore, R., Karnieli, A., O'Neill, N. T., Pietras, C., Pinker, R. T., Voss, K., and Zibordi, G.: An emerging ground-based aerosol climatology: Aerosol Optical Depth from AERONET, Geophys. Res., 106(12), 12067–12097, 2001.

IPCC, Intergovernmental Panel on Climate Change: Climate change 2001: Aerosols, their direct and indirect effects, Cambridge Univ. Press, New York, 881 pp., 2001.

IPCC, Intergovernmental Panel on Climate Change: Climate change 2007: Synthesis Report, [http://www.ipcc.ch/pdf/assessment-report/ar4/syr/ar4\\_syr.pdf](http://www.ipcc.ch/pdf/assessment-report/ar4/syr/ar4_syr.pdf), 2007.

Jiménez, P., Jorba, O., Parra, R., and Baldasano, J. M.: Evaluation of MM5-EMICAT2000-CMAQ performance and sensitivity in complex terrain: High-resolution application to the northeastern Iberian Peninsula, Atmos. Environ., 40(26), 5056–5072, 2006.

Kaskaoutis, D. G., Kambezidis, H. D., Hatzianastassiou, N., Kosmopoulos, P. G., and Badarinarath, K. V. S.: Aerosol climatology: on the discrimination of aerosol types over four AERONET sites, Atmos. Chem. Phys. Discuss., 7, 6357–6411, 2007, <http://www.atmos-chem-phys-discuss.net/7/6357/2007/>.

Kaufman, Y. J.: Aerosol optical thickness and atmospheric path radiance, J. Geophys. Res,

98(D2), 2677–2692, 1993.

Kim, S. W., Yoon, S. C., Kim, J., and Kim, S. Y.: Seasonal and monthly variations of columnar aerosol optical properties over east Asia determined from multi-year MODIS, LIDAR, and AERONET Sun/sky radiometer measurements, *Atmos. Environ.*, 41(8), 1634–1651, 2007.

5 Kubilay, N., Nickovic, S., Moulin, C., and Dulac, F.: An illustration of the transport and deposition of mineral dust onto the eastern Mediterranean, *Atmos. Environ.*, 34, 1293–1303, 2000.

Kubilay, N., Cokacar, T., and Oguz, T.: Optical properties of mineral dust outbreaks over the northeastern Mediterranean, *J. Geophys. Res.*, 108(D21), 4666, 2003.

10 Lelieveld, J., Berresheim, H., Borrmann, S., Crutzen, P. J., Dentener, F. J., Fischer, H., Feichter, J., Flatau, P. J., Heland, J., Holzinger, R., Korrmann, R., Lawrence, M. G., Levin, Z., Markowicz, K. M., Mihalopoulos, N., Minikin, A., Ramanathan, V., Reus, M. d., Roelofs, G. J., Scheeren, H. A., Sciare, J., Schlager, H., Schultz, M., Siegmund, P., Steil, B., Stephanou, E. G., Stier, P., Traub, M., Warneke, C., Williams, J., and Ziereis, H.: Global Air Pollution Crossroads over the Mediterranean, *Science*, 298(5594), 794–799, 2002.

15 Levin, Z., Ganor, E., and Gladstein, V.: The effects of desert particles coated with sulfate on rain formation in the eastern Mediterranean, *Appl. Meteorol.*, 35(9), 1511–1523, 1996.

Liu, M., Westphal, D. L., Holt, T. R., and Xu, Q.: Numerical Simulation of a Low-Level Jet over Complex Terrain in Southern Iran, *Mon. Weather Rev.*, 128(5), 1309–1327, 2000.

20 Martín Vide, J.: Interpretación de los mapas del tiempo, Ketres Editora SA, Barcelona, 170 pp., 1984.

Middleton, N. J. and Goudie, A. S.: Saharan dust: sources and trajectories, *Trans. Inst. Br. Geogr.*, 26(2), 165, 2001.

25 Moulin, C., Lambert, C. E., Dayan, U., Masson, V., Ramonet, M., Bousquet, P., Legrand, M., Balkanski, Y. J., Guelle, W., Marticorena, B., Bergametti, G., and Dulac, F.: Satellite climatology of African dust transport in the Mediterranean atmosphere, *J. Geophys. Res.*, 103(D11), 13137–13144, 1998.

O'Neill, N. T., Dubovik, O., and Eck, T. F.: A modified Angstrom coefficient for the characterization of sub-micron aerosols, *Appl. Optics*, 40(14), 2368–2375, 2001.

30 O'Neill, N. T., Eck, T. F., Smirnov, A., Holben, B. N., and Thulasiraman, S.: Spectral discrimination of coarse and fine mode optical depth, *J. Geophys. Res.*, 108, 4559, 2003.

O'Neill, N. T.: Comment on “Classification of aerosol properties derived from AERONET direct sun data” by G. P. Gobbi et al. (2007)”, *Atmos. Chem. Phys. Discuss.*, 9, 175–182, 2009, <http://www.atmos-chem-phys-discuss.net/9/175/2009/>.

**Aerosol  
characterization in  
N-Africa, NE-Atlantic,  
M. Basin and M. East**

S. Basart et al.

Title Page

Abstract

Introduction

Conclusions

References

Tables

Figures

◀

▶

◀

▶

Back

Close

Full Screen / Esc

Printer-friendly Version

Interactive Discussion

- Ogunjobi, K., Ajayi, V., Balogun, I., Omotosho, J., and He, Z.: The synoptic and optical characteristics of the harmattan dust spells over Nigeria, *Theor. Appl. Climatol.*, 93(1), 91–105, 2008.
- Pace, G., Sarra, A. d., Meloni, D., Piacentino, S. and Chamard, P.: Aerosol optical properties at Lampedusa (Central Mediterranean). 1. Influence of transport and identification of different aerosol types, *Atmos. Chem. Phys.*, 6, 697–713, 2006, <http://www.atmos-chem-phys.net/6/697/2006/>.
- Pappalardo, G., Amodeo, A., Amoruso, S., Mona, L., Pandolfi, M., and Cuomo, V.: One year of tropospheric lidar measurements of aerosol extinction and backscatter, *Ann. Geophys.*, 46(2), 401–413, 2003.
- Pérez, C., Sicard, M., Jorba, O., Comerón, A., and Baldasano, J. M.: Summertime recirculations of air pollutants over the north-eastern Iberian coast observed from systematic EARLINET lidar measurements in Barcelona, *Atmos. Environ.*, 38, 3983–4000, 2004.
- Perrone, M. R., Santese, M., Tafuro, A. M., Holben, B., and Smirnov, A.: Aerosol load characterization over South-East Italy for one year of AERONET sun-photometer measurements, *Atmos. Res.*, 75(1–2), 111–133, 2005.
- Prospero, J. M., Schmitt, R., Cuevas, E., Savoie, D., Graustein, W., Turekian, K., Volz-Thomas, A., Diaz, A., Oltmans, S., and Levy-II, H.: Temporal Variability of Summer-time Ozone and Aerosols in the Free Troposphere over the Eastern North Atlantic, *J. Geophys. Res. Lett.*, 22(21), 2925–2928, 1995.
- Prospero, J. M., Ginoux, P., Torres, O., Nicholson, S. E., and Gill, T. E.: Environmental characterization of global sources of atmospheric soil dust identified with the nimbus 7 total ozone mapping spectrometer (TOMS) absorbing aerosol product, *Rev. Geophys.*, 40(1), 1002, 2002.
- Querol, X., Alastuey, A., Rodríguez, S., Viana, M., Artiano, B., Salvador, P., Mantilla, E., Santos, S. G. d., Patier, R. F., Rosa, J. d. L., Campa, A. S. d. I., Menendez, M., and Gil, J. J.: Levels of particulate matter in rural, urban and industrial sites in Spain, *Sci. Total Environ.*, 334–335, 359–376, 2004.
- Reid, J. S., Eck, T. F., Christopher, S. A., Hobbs, P. V., and Holben, B.: Use of the Ångström exponent to estimate the variability of optical and physical properties of aging smoke particles in Brazil, *Geophys. Res.*, 104(D22), 27473–27490, 1999.
- Remer, L. and Kaufman, Y. J.: Dynamic aerosol model- Urban/industrial aerosol, *J. Geophys. Res.*, 103(D12), 13859–13871, 1998.

---

**Aerosol  
characterization in  
N-Africa, NE-Atlantic,  
M. Basin and M. East**S. Basart et al.

---

[Title Page](#)[Abstract](#)[Introduction](#)[Conclusions](#)[References](#)[Tables](#)[Figures](#)[◀](#)[▶](#)[◀](#)[▶](#)[Back](#)[Close](#)[Full Screen / Esc](#)[Printer-friendly Version](#)[Interactive Discussion](#)

- Rodríguez, S. and Guerra, J. C.: Monitoring of ozone in a marine environment in Tenerife (Canary Islands), *Atmos. Environ.*, 135, 1829–1841, 2001.
- Rodríguez, S., Querol, X., Alastuey, A., Kallos, G., and Kakaliagou, O.: Saharan dust contributions to PM<sub>10</sub> and TSP levels in Southern and Eastern Spain, *Atmos. Environ.*, 35, 2433–2447, 2001.
- Rodríguez, S., Cuevas, E., González, Y., Ramos, R., Romero, P. M., Pérez, N., Querol, X., and Alastuey, A.: Influence of sea breeze circulation and road traffic emissions on the relationship between particle number, black carbon, PM<sub>1</sub>, PM<sub>2.5</sub> and PM<sub>2.5–10</sub> concentrations in a coastal city, *Atmos. Environ.*, 42, 6523–6534, 2008.
- Schuster, G. L., Dubovik, O., and Holben, B. N.: Angstrom exponent and bimodal aerosol size distributions, *J. Geophys. Res.*, 111, D07207, doi:10.1029/2005JD006328, 2006.
- Sciare, J., Bardouki, H., Moulin, C., and Mihalopoulos, N.: Aerosol sources and their contribution to the chemical composition of aerosols in the Eastern Mediterranean Sea during summertime, *Atmos. Chem. Phys.*, 3, 291–302, 2003, <http://www.atmos-chem-phys.net/3/291/2003/>.
- Silva, A., Costa, M., Elias, T., Formenti, P., Belo, N., and Pereira, S.: Ground-based aerosol monitoring at Évora, Portugal, *Global Change NewsLetter*, 56, December, 2003.
- Smirnov, A., Holben, B. N., Eck, T. F., Dubovik, O., and Slutsker, I.: Cloud screening and quality control algorithms for the AERONET database, *Rem. Sens. Environ.*, 73, 337–349, 2000.
- Smirnov, A., Holben, B. N., Eck, T. F., Slutsker, I., Chatenet, B., and Pinker, R. T.: Diurnal variability of aerosol optical depth observed at AERONET (Aerosol Robotic Network) sites, *J. Geophys. Res. Lett.*, 29(23), 2115, 2002a.
- Smirnov, A., Holben, B. N., Dubovik, O., O'Neill, N. T., Eck, T. F., Westphal, D. L., Gorch, A. K., Pietras, C., and Slutsker, I.: Atmospheric Aerosol Optical Properties in the Persian Gulf, *Atmos. Sci.*, 59, 620–634, 2002b.
- Sultan, B., Labadi, K., Guegan, J. F., and Janicot, S.: Climate drives the meningitis epidemics onset in West Africa, *PLoS Medicine*, 2(1), doi:10.1371/journal.pmed.0020006, 2005.
- Toledano, C., Cachorro, V. E., Berjon, A., de Frutos, A. M., Sorribas, M., de la Morena, B. A., and Goloub, P.: Aerosol optical depth and Angstrom exponent climatology at El Arenosillo AERONET site (Huelva, Spain), *Q. J. Roy. Meteor. Soc.*, 133, 795–807, doi:10.1002/qj54, 2007.
- Torres, C., Cuevas, E., and Guerra, J. C.: Caracterización de la capa de mezcla marítima y de la atmósfera libre en la región subtropical sobre Canarias., *Asemblea Hispano Portuguesa*

---

**Aerosol  
characterization in  
N-Africa, NE-Atlantic,  
M. Basin and M. East**S. Basart et al.

---

Title Page

Abstract

Introduction

Conclusions

References

Tables

Figures

◀

▶

◀

▶

Back

Close

Full Screen / Esc

Printer-friendly Version

Interactive Discussion

de Geodesia y Geofísica, Valencia, 2002.  
Viana, M., Querol, X., Alastuey, A., Cuevas, E., and Rodríguez, S.: Influence of African dust on the levels of atmospheric particulates in the Canary Islands air quality network, Atmos. Environ., 36, 5861–5875, 2002.

ACPD

9, 7707–7745, 2009

---

**Aerosol  
characterization in  
N-Africa, NE-Atlantic,  
M. Basin and M. East**

S. Basart et al.

---

Title Page

Abstract

Introduction

Conclusions

References

Tables

Figures

◀

▶

◀

▶

Back

Close

Full Screen / Esc

Printer-friendly Version

Interactive Discussion

7735



**Table 1.** Location and description of the selected AERONET stations. Class of location which are defined as stations: above 1000 m (H), in arid and desert areas (D), in the ocean (O), in remote and urban areas (R/U) and in littoral areas (C); coordinates, altitude, first and last measurement date, the number of total measurements (Dataset), the number of days (N) and months (Mo.) in the observation periods, and the percentage of cloud screened data of the selected AERONET stations.

AERONET site	CODE	Class	LAT (°/N)	LON(°/W)	ALT(m)	First data	Last data	Dataset	N	Mo.	Cloud screened
North-Western Africa											
Agoufou	AGO	D	15.345	-1.4791	305	25/09/2003	31/05/2007	39 530	1147	45	30.88
Banizoumbou	BAN	D	13.541	2.6648	250	16/10/1995	05/07/2007	77 529	2575	108	36.20
Capo Verde	CVR	O	16.733	-22.935	60	21/10/1994	11/04/2007	46 216	2496	125	39.29
Dahkla	DAH	R/UC	23.717	-15.95	12	13/02/2002	05/11/2003	18 789	563	22	25.70
Dakar	DAK	R/UC	14.394	-16.959	0	04/12/1996	12/10/2006	38 454	1387	69	33.91
Djougou	DJO	R/U	9.7601	1.599	400	24/02/2004	07/05/2007	22 012	819	36	34.99
IER Cinzana	CIN	D	13.278	-5.9339	285	01/06/2004	26/05/2007	33 207	971	36	31.09
Ilorin	ILO	R/U	8.32	4.34	350	25/04/1998	27/05/2006	23 556	1307	66	38.45
Izana	IZO	HO	28.3	-16.5	2367	17/06/1997	16/10/2006	26 995	690	31	37.51
Ouagadougou	OUA	D	12.2	-1.4	290	01/01/1995	15/03/2005	44 820	1779	74	38.20
Saada	SAA	D	31.626	-8.1558	420	01/07/2004	02/06/2006	19 512	509	21	25.64
Santa Cruz Tenerife	SCO	O	28.473	-16.247	52	15/07/2005	07/05/2007	11 487	449	23	36.40
Iberian Peninsula and Mediterranean Basin											
Avignon	AVI	R/U	43.933	4.8781	32	08/12/1999	26/06/2006	41 605	1548	77	33.84
Barcelona	BCN	R/UC	41.386	2.117	125	16/12/2004	24/05/2006	9 457	357	18	37.60
Blida	BLI	R/UC	36.508	2.8806	230	30/10/2003	16/11/2006	15 573	701	37	33.94
Cabo da Roca	ROC	R/UC	38.783	-9.5	140	10/12/2003	27/02/2007	11 774	551	32	37.14
Cairo EMA	CAI	R/U	30.081	31.29	70	13/04/2005	23/03/2006	5 012	269	12	54.79
Carpentras	CAR	R/U	44.083	5.0583	100	18/02/2003	24/10/2007	35 308	1177	54	33.93
El Arenosillo	ARE	R/UC	37.105	-6.7335	0	16/02/2000	12/06/2006	39 380	1344	61	26.75
Evora	EVO	R/U	38.568	-7.9115	293	03/07/2003	09/07/2006	24 470	749	34	28.33

## Aerosol characterization in N-Africa, NE-Atlantic, M. Basin and M. East

S. Basart et al.

Title Page

Abstract

Introduction

Conclusions

References

Tables

Figures

⏪

⏩

◀

▶

Back

Close

Full Screen / Esc

Printer-friendly Version

Interactive Discussion

Table 1. Continued.

AERONET site	CODE	Class	LAT (°N)	LON(°W)	ALT(m)	First data	Last data	Dataset	N	Mo.	Cloud screened
Iberian Peninsula and Mediterranean Basin											
Forth Crete	CRE	R/UC	35.333	25.282	20	04/01/2003	06/11/2006	33625	1072	47	23.65
Granada	GRA	R/UC	37.164	−3.605	680	29/12/2004	11/11/2007	20882	631	29	32.75
IMC Oristano	ORI	R/UC	39.91	8.5	10	30/05/2000	21/10/2003	24251	934	42	26.70
IMS-METU-Erdemli	ERD	R/UC	36.565	34.255	3	12/11/1999	03/05/2006	34910	1218	57	24.23
Lampedusa	LAM	R/UC	35.517	12.632	45	27/06/2000	12/06/2006	17361	813	39	22.46
Lecce University	LEC	R/U	40.335	18.111	30	08/03/2003	28/11/2006	26361	988	42	32.04
Nes Ziona	ZIO	R/U	31.922	34.789	40	24/02/2000	21/11/2006	42077	1577	72	31.08
Palencia	PAL	R/U	41.989	−4.5157	750	23/01/2003	24/05/2006	22220	796	39	32.48
Rome Tor Vergata	ROM	R/U	41.84	12.647	130	15/02/2001	20/12/2006	33773	1310	62	35.24
Sede Boker	SED	D	30.855	34.782	480	25/01/1996	20/10/2007	80901	2549	110	27.96
Thessaloniki	THE	R/UC	40.63	22.96	60	03/09/2005	06/05/2007	12883	426	21	30.09
Toulon	TUL	R/UC	43.136	6.0094	50	15/11/2004	16/05/2007	20054	703	31	32.97
Villefranche	VIL	R/UC	43.684	7.3289	130	07/01/2004	19/01/2007	19431	643	31	32.45
Middle East											
Bahrain	BHR	R/UC	26.208	50.609	25	23/07/1998	02/10/2006	28936	1117	49	23.71
Dhabi	DHA	R/UC	24.481	54.383	15	05/10/2003	30/09/2007	27601	791	30	27.18
Dhadnah	DHD	R/UC	25.513	56.325	81	28/06/2004	21/09/2007	40494	1046	40	22.29
Hamim	HMM	D	22.967	54.3	209	22/06/2004	07/08/2007	27094	876	37	23.73
Mussafa	MUS	R/UC	24.372	54.467	10	04/10/2004	14/03/2006	17892	480	18	30.19
Solar Village	SVI	D	24.907	46.397	764	22/02/1999	12/11/2006	87802	2259	87	24.00

## Aerosol characterization in N-Africa, NE-Atlantic, M. Basin and M. East

S. Basart et al.

Title Page

Abstract

Introduction

Conclusions

References

Tables

Figures

⏪

⏩

◀

▶

Back

Close

Full Screen / Esc

Printer-friendly Version

Interactive Discussion

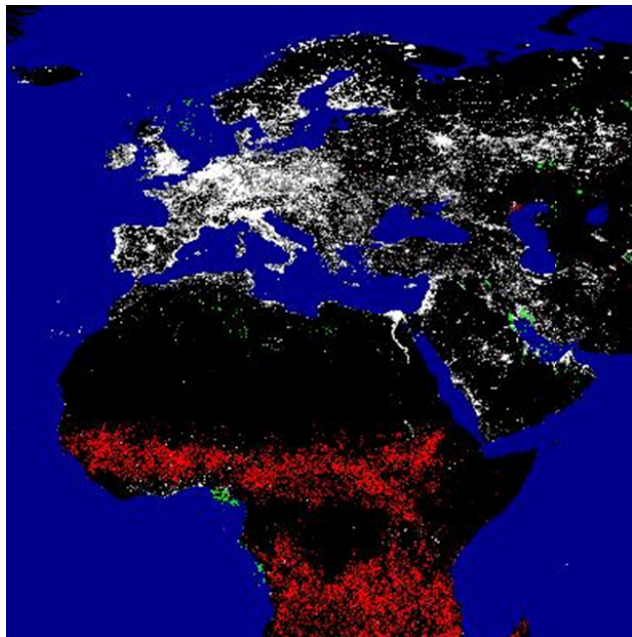


**Fig. 1.** DMSM Nighttime Lights. Produced using cloud-free portions of low-light imaging data acquired by the US Air Force Defense Meteorological Satellite Program (DMSM) Operational Linescan System (OLS). Four primary types of lights were identified: human settlements – cities, towns, and villages (white), fires (red), gas flares (green), and heavily lit fishing boats (blue). The four types of lights were distinguished from each other based on their appearance, persistence and location. Fires were identified as ephemeral lights on land. Lights from human settlements occur on land and are persistent over time. Gas flares are extremely bright, have a circular appearance, and have no major city present when cross referenced against an atlas. The heavily lit fishing boats are collections of lights found in certain ocean areas and are primarily the result of squid fishing. Date range covers 1 January – 31 December 2003. Data analysis and digital image creation by NOAA-NESDIS-National Geophysical Data Center-Earth Observations Group Boulder, Colorado USA (<http://www.ngdc.noaa.gov/dmsp>).

**Aerosol  
characterization in  
N-Africa, NE-Atlantic,  
M. Basin and M. East**

S. Basart et al.

Title Page

Abstract

Introduction

Conclusions

References

Tables

Figures



Back

Close

Full Screen / Esc

Printer-friendly Version

Interactive Discussion





## Aerosol characterization in N-Africa, NE-Atlantic, M. Basin and M. East

S. Basart et al.

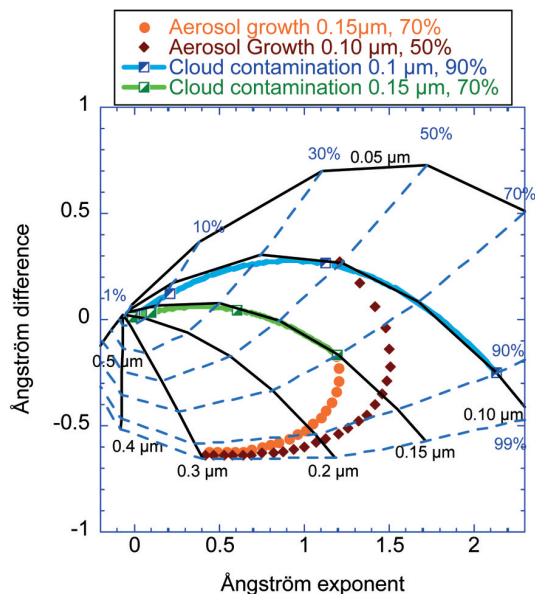


**Fig. 3.** Simulations of the classification of the aerosol properties as a function of the Ångström exponent  $\alpha$  (440, 870) and the difference  $\delta\alpha = \alpha(440, 675) - \alpha(675, 870)$ , for bimodal, lognormal size distributions with refractive index  $m = 1.4 - 0.001i$  extracted from Gobbi et al. (2007). The black solid lines are each for a fixed size of the fine mode  $R_f$  and the dashed blue lines for a fixed fraction contribution  $\eta$  of the fine mode to the AOD at 675 nm. Split squares represent the effects of a cloud contamination of 0, 50, 90 and 99% in the AOD of two grid points: 1)  $\eta = 70\%$ ,  $R_f = 0.15 \mu\text{m}$  (bright green line) and 2)  $\eta = 90\%$ ,  $R_f = 0.1 \mu\text{m}$  (turquoise line). This contamination results in a departure from the original grid points along the constant  $R_f$  lines and towards the origin. Conversely, hydration of the aerosol fine mode (two starting conditions simulated: 1)  $\eta = 50\%$ ,  $R_f = 0.1 \mu\text{m}$  (brown diamonds), and 2)  $\eta = 70\%$ ,  $R_f = 0.15 \mu\text{m}$  (orange circles)) is accompanied by a movement towards the origin along the opposite direction, with concurrent increase in  $R_f$  and  $\eta$ .

Title Page

Abstract

Introduction

Conclusions

References

Tables

Figures

⏪

⏩

◀

▶

Back

Close

Full Screen / Esc

Printer-friendly Version

Interactive Discussion

## Aerosol characterization in N-Africa, NE-Atlantic, M. Basin and M. East

S. Basart et al.

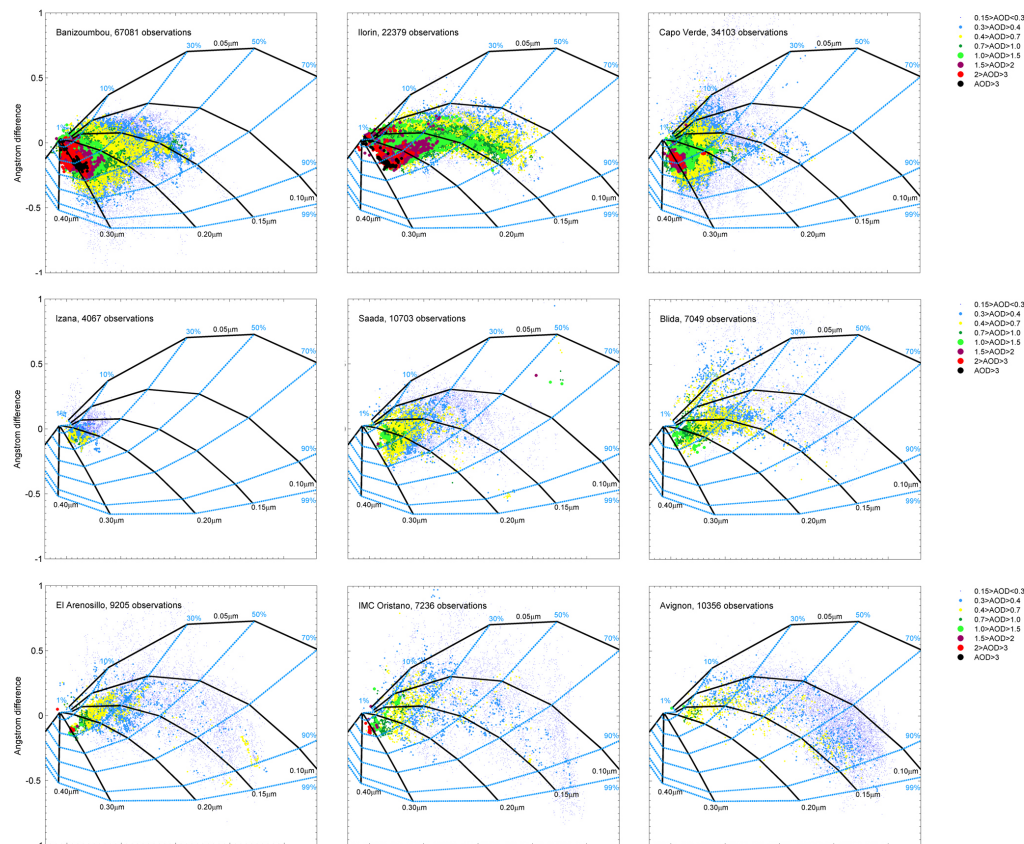


**Fig. 4.** Ångström exponent difference,  $\delta\alpha = \alpha(440, 675) - \alpha(675, 870)$ , as a function of the 440–870 nm Ångström exponent and AOD at 675 nm (color code) for fifteen AERONET stations (from top): Banizoumbou, Ilorin, Capo Verde, Saada, Izana, Blida, El Arenosillo, IMC Oristano, Avignon, Rome Tor Vergata, Thessaloniki, Lampedusa, Nes Ziona, Mussafa and Hammim.

[Title Page](#)
[Abstract](#)
[Introduction](#)
[Conclusions](#)
[References](#)
[Tables](#)
[Figures](#)
[⏪](#)
[⏩](#)
[⏴](#)
[⏵](#)
[Back](#)
[Close](#)
[Full Screen / Esc](#)
[Printer-friendly Version](#)
[Interactive Discussion](#)

## Aerosol characterization in N-Africa, NE-Atlantic, M. Basin and M. East

S. Basart et al.

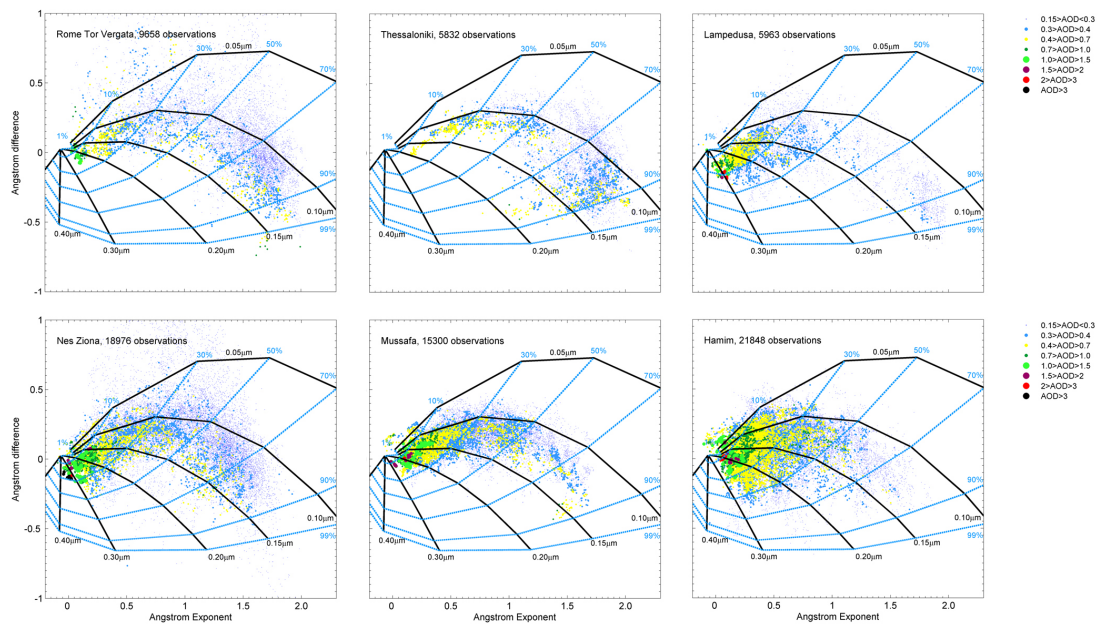
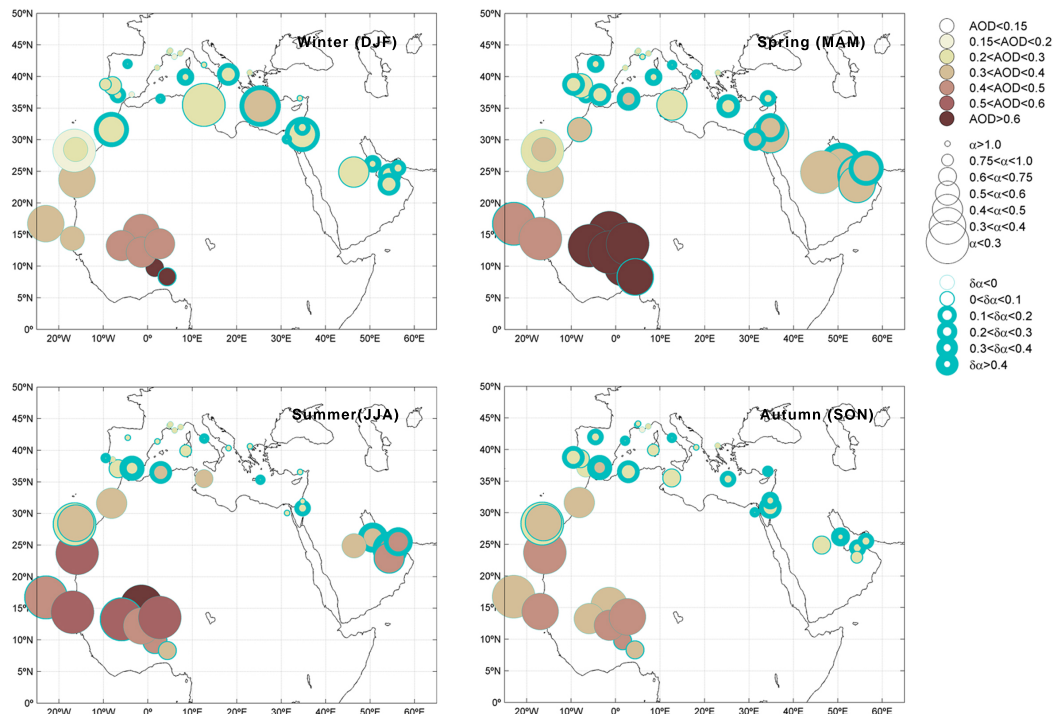


Fig. 4. Continued.

[Title Page](#)
[Abstract](#)
[Introduction](#)
[Conclusions](#)
[References](#)
[Tables](#)
[Figures](#)
[Back](#)
[Close](#)
[Full Screen / Esc](#)
[Printer-friendly Version](#)
[Interactive Discussion](#)

## Aerosol characterization in N-Africa, NE-Atlantic, M. Basin and M. East

S. Basart et al.



**Fig. 5.** Seasonal mean of all available measurements with AOD > 0.15 for all selected AERONET stations: AOD at 675 nm (colour code),  $\alpha(440, 870)$  (size code) and Ångström exponent difference,  $\delta\alpha = \alpha(440, 675) - \alpha(675, 870)$  (blue contour code).

[Title Page](#)
[Abstract](#)
[Introduction](#)
[Conclusions](#)
[References](#)
[Tables](#)
[Figures](#)
[⏪](#)
[⏩](#)
[◀](#)
[▶](#)
[Back](#)
[Close](#)
[Full Screen / Esc](#)
[Printer-friendly Version](#)
[Interactive Discussion](#)

## Aerosol characterization in N-Africa, NE-Atlantic, M. Basin and M. East

S. Basart et al.

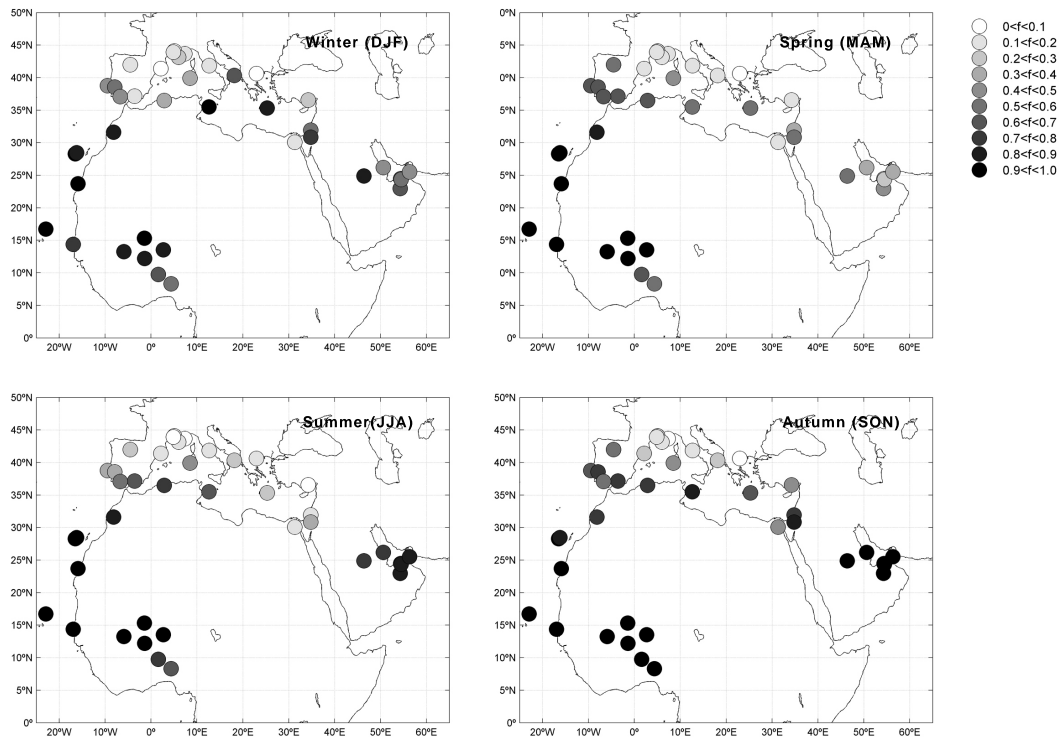


**Fig. 6.** Seasonal frequency of large aerosols ( $AOD > 0.15$  and  $\alpha < 0.75$ ) respect to total number of measurements with  $AOD > 0.15$  for all selected AERONET stations, being 0 when no large aerosols are observed and 1 when all dataset are concentrated in this coarse fraction.

[Title Page](#)
[Abstract](#)
[Introduction](#)
[Conclusions](#)
[References](#)
[Tables](#)
[Figures](#)
[◀](#)
[▶](#)
[◀](#)
[▶](#)
[Back](#)
[Close](#)
[Full Screen / Esc](#)
[Printer-friendly Version](#)
[Interactive Discussion](#)

## Aerosol characterization in N-Africa, NE-Atlantic, M. Basin and M. East

S. Basart et al.

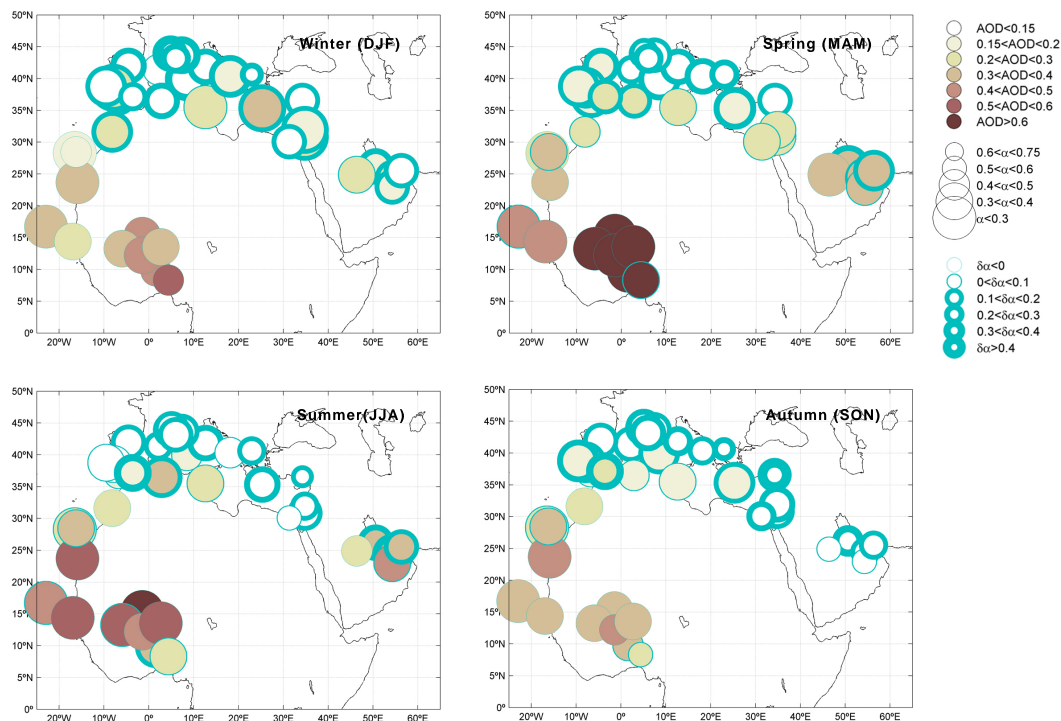


**Fig. 7.** Seasonal mean contribution to AOD of large aerosols (AOD > 0.15 and  $\alpha < 0.75$ ) and their corresponding  $\alpha$  and  $\delta\alpha$  seasonal averages for all selected AERONET: AOD at 675 nm (colour code),  $\alpha(440, 870)$  (size code) and Ångström exponent difference,  $\delta\alpha = \alpha(440, 675) - \alpha(675, 870)$  (blue contour code).

Title Page

Abstract

Introduction

Conclusions

References

Tables

Figures

◀

▶

◀

▶

Back

Close

Full Screen / Esc

Printer-friendly Version

Interactive Discussion